# FIXATION TIMES IN GRAPH-STRUCTURED POPULATIONS

## Fixierungszeiten in Populationen mit Graphenstruktur

**MASTERARBEIT**

im Rahmen des Studiengangs
**Mathematik in Medizin und Lebenswissenschaften**
der Universität zu Lübeck

vorgelegt von
**Laura Hindersin**

ausgegeben und betreut von
**Prof. Dr. Arne Traulsen**

Die Masterarbeit ist im Rahmen einer Tätigkeit in der Forschungsgruppe Evolutionstheorie des Max-Planck-Instituts für Evolutionsbiologie in Plön entstanden.

Lübeck, den 06. November 2013

# Eidesstattliche Erklärung

Ich versichere an Eides statt, dass ich die vorliegende Arbeit selbständig verfasst und keine anderen als die angegebenen Quellen und Hilfsmittel benutzt habe. Die aus fremden Quellen direkt oder indirekt übernommenen Gedanken sind als solche gekennzeichnet. Die Arbeit wurde bisher in gleicher oder ähnlicher Form keiner anderen Prüfungsbehörde vorgelegt und auch nicht veröffentlicht.

---

Ort/Datum

---

Unterschrift

# Abstract

The Moran process is widely used for modeling stochastic dynamics of finitely large populations. It describes the invasion process of a novel mutant into a resident population. Generally, the population is assumed to be well-mixed, which is a rather strong assumption. Studying the Moran process on graphs instead of unstructured populations is a recent approach to overcome this assumption. Some graph structures increase the fixation probability of a mutant that has a fitness advantage compared to the resident population. Graphs with this property are called amplifiers of selection. However, simulations show that the time until fixation increases considerably on those graphs.

The objective of this thesis is to analyze different graphs of small size with respect to the fixation time. Simulations support the results for larger population size, where analytical approaches are unfeasible. We show that depending on the initial graph structure, the removal of one link can either lead to an increase or decrease in fixation time. This result is surprising and counterintuitive. Another interesting finding is that the shortest average fixation time does not only depend on the mutant's starting node. But instead, different starting nodes are preferable, depending on the mutant's fitness.

# Zusammenfassung

Der Moran-Prozess ist weit verbreitet in der Modellierung stochastischer Dynamik von endlich großen Populationen. Er beschreibt die Invasion einer neuen Mutante in eine bestehende Population. Im Allgemeinen wird die Population als gut gemischt angenommen, welches eine ziemlich starke Annahme darstellt. Ein neuer Ansatz untersucht den Moran-Prozess auf Graphen, statt auf unstrukturierten Populationen, um auf diese Annahme verzichten zu können. Einige Graphen erhöhen die Fixierungswahrscheinlichkeit eines Mutanten, der einen Fitness-Vorteil im Vergleich zur bestehenden Population hat. Graphen mit dieser Eigenschaft werden Selektionsverstärker genannt. Simulationen zeigen jedoch, dass die Zeit bis zur Fixierung auf diesen Graphen deutlich erhöht ist.

Das Ziel dieser Arbeit ist es, die Fixierungszeit verschiedener kleiner Graphen zu analysieren. Simulationen unterstützen die Ergebnisse für größere Populationen, wo analytische Ansätze undurchführbar sind. Wir zeigen, dass das Weglassen eines Links von einem Graphen die Fixierungszeit entweder erhöhen oder erniedrigen kann. Dieses Ergebnis ist überraschend und kontraintuitiv. Ein weiteres interessantes Ergebnis ist, dass die kürzeste durchschnittliche Fixierungszeit nicht nur von der Anfangsposition des Mutanten abhängt, sondern auch, dass unterschiedliche Anfangspositionen vorteilhaft sind, je nach Fitness des Mutanten.

# Contents

# List of Figures

# List of Tables

# 1 Introduction

Modeling stochastic population dynamics usually assumes a panmixia of individuals, where the probability of meeting and therefore interacting is the same for everyone. But most populations do not live in a permanently stirred liquid. Instead, the environment has a crucial effect on interaction and reproduction. Some individuals may never meet, due to spatial structure.
Additional to the topology of the habitat, the social structure often has an impact on population dynamics. Therefore, the assumption of a well-mixed population is not appropriate in many cases. This is why the present thesis focusses on structured populations.

We study the Moran process on graph-structured populations, as established by *Lieberman et al.* [2005], where individuals inhabit the nodes of a graph of fixed size [see *Nowak*, 2006; *Broom and Rychtář*, 2008]. Links between nodes determine into which nodes the individuals place their offspring during the birth-death process.
Individuals have a fitness, influencing the probability to place offspring into their neighboring nodes. Therefore, fitness determines reproductive success.
At the beginning of the process, a single individual of type $A$, a so called mutant, with a fitness value $r > 0$ is introduced into a population of $N - 1$ individuals of wild type $B$ with fitness one. A fitness $r > 1$ means that the mutant is advantageous compared to the residents, whereas $r < 1$ yields a disadvantage and $r = 1$ corresponds to neutral evolution. At every time step, one individual is chosen for birth with probability proportional to fitness. It produces one identical offspring to replace one randomly chosen neighbor.
Here links are undirected, which means that both neighbors sharing one link can replace the other one. But the probabilities of replacement are different in general, since they depend on the individual's fitness and on the degree of the node, which is the number of neighbors.

As a first property of interest, the fixation probability is usually examined. This is the probability for one single mutant to invade and take over the whole population. Even though a mutant might be advantageous, fixation is of course a matter of probabilities. Random drift occurs, sometimes even leading to the extinction of highly advantageous mutants. In a large population, the fixation probability for advantageous mutants is approximately $1 - \frac{1}{r}$ , therefore a mutant being twice as fit as the residents, still has only a probability of $\frac{1}{2}$ to succeed [*Nowak*, 2006]. In the absence of mutations, fixation and extinction are absorbing states of the process.

Stochastic population dynamics are often modeled as Markov chains [*Karlin and Taylor*, 1975; *Allen*, 2003], because only the current composition of the population determines the probability of the composition in the future. The previous states do not matter. Therefore, we start by recapturing discrete time Markov chains. A nice approach, explained by *Grinstead and Snell* [1997], for calculating the absorption probability and time of a Markov chain is stated. To introduce the spatial population structure on which the process occurs, some basics of graph theory are specified.

The introduction of spatial population structure can change the fixation probability [*Lieberman et al.*, 2005; *Nowak*, 2006]. For example in a star-like structure, where one center node is connected to all leaf nodes, a mutant with fitness $r$ has the same fixation probability as a mutant with fitness $r^2$ in a well-mixed population of the same size. Such structures, that increase the fixation probability for advantageous mutants and decrease it for disadvantageous ones, are termed amplifiers of selection [*Traulsen et al.*, 2005].

Suppressors of selection, on the other hand, are graphs that decrease the fixation probability for advantageous mutants and increase it for disadvantageous mutants. On regular graphs, where every node has the same number of neighbors, the fixation probability is the same as in the well-mixed population. Since all nodes have the same potential to change their state, graphs with this property are called isothermal. Examples for isothermal graphs are the one and two-dimensional lattice with periodic boundary conditions. The one-dimensional lattice is also called a ring. Obviously the well-mixed population, where the node degree is equal to the population size minus one for all nodes, is also isothermal. We will refer to the well-mixed population as the complete graph as well, since it has the maximum number of links that are possible in a graph without allowing self-links.

Another interesting property of the process is the fixation time. How many time steps does a single mutant need on average to take over the whole population? It turns out that many irregular graphs increase fixation time, compared to the well-mixed population. But even the isothermal ring increases fixation time.

Selection is constant in our setting, since individual fitness does not depend on the composition of the population. Frequency dependent selection is modeled on graphs as well [see *Nowak and May*, 1992; *Abramson and Kuperman*, 2001; *Santos and Pacheco*, 2005; *Ohtsuki et al.*, 2006; *Nowak et al.*, 2010]. In this evolutionary game theory on graphs, individuals on the nodes interact with their neighbors. For example, each individual plays a game with his neighbors. After every round, the individuals are replaced by the type of the one neighbor that achieved the highest payoff. Therefore, individual payoff in the game depends on the frequency of the types (or strategies) at all adjacent nodes and is translated into fitness. But since fixation time on graphs is already difficult to derive for constant selection, we restrict ourselves to the latter.

The increase in probability on the above-mentioned stars has led to the following question: "Does fixation occur at a higher rate on the star compared to the well-mixed population?".
*Frean et al.* [2013] addressed this question. Formerly, the rate of evolution was considered as $N\mu\Phi_1^N$ , which is the population size times the mutation rate times the fixation probability of one single mutant [*Ewens*, 2004]. This corresponds to the rate at which a successful mutant appears, assuming that waiting for that mutant takes much longer than its time to fixation. But since some graph structures increase fixation time considerably, the assumption is not valid anymore and fixation time should be included into the rate of evolution.
Therefore *Frean et al.* [2013] introduced the effective rate of evolution as the harmonic mean of those two rates. They have shown that the effect of graph structure on fixation time is not negligible for the effective rate of evolution (at least for intermediate mutation rates, see chapter 2.3.5 below).

We will therefore analyze different graph structures and their respective fixation time more closely. So far, it is not clear what effect the removal of links from a graph has on fixation time. Simulations suggest that the removal of one link from the well-mixed population always increases

fixation time. The aim of this thesis is to prove this analytically.

Trying that leads to some non-intuitive results. Chapter 3 analyzes all different graph structures of size four in terms of the fixation probability and time, sojourn time and initial mutant placement. We show analytically and with simulations, that removing one link from a graph can increase fixation time, but removing a second link can decrease it again.
Additionally, we will put the first mutant at a specific node, instead of the random placement we used before, to get a better understanding of the influence of graph structure on fixation time. Studying initial mutant placement yields some surprising results as well. As it turns out, not only does the position of the first mutant change the shortest average fixation time. Instead, the starting node which leads to the fastest fixation depends on the fitness of the mutant. For a slight fitness advantage, starting at a specific node can shorten fixation time, whereas for a higher fitness, another starting node might be preferable.

In chapter 4, simulations on graphs of size eight are visualized. As expected, the ring and the star again show a very high fixation time. We remove up to three links from the complete graph of size eight. Dropping one, two or three links leads to a slight increase in fixation time.
There are five possible ways to remove three links in a graph of size eight. By observing those five structures, it seems that the more isolated a node is, the more the fixation time on that graph increases (see chapter 5 for a discussion about variance of node degree).
Additionally, the non-intuitive result from chapter 3 is analyzed in larger graphs.

So far we focussed on the mean fixation time. Finally, the outlook in chapter 5.2 takes the whole distribution into account. Additional simulations show that the distributions of fixation time are right-skewed, meaning that fixation time is often short but with many outliers that take a very long time.

# 2 Background and Methods

The process of mutant invasion into a population is often modeled as a Markov chain. At first we define Markov chains and their transition matrices [see *Karlin and Taylor*, 1975; *Allen*, 2003]. Then an approach for calculation of the absorption probability and time of a Markov chain by *Grinstead and Snell* [1997] is described.

## 2.1 Markov Chains

### 2.1 Definition
*Let $X := \{X_n\}$, $n \in \mathbb{N}_0$, be a discrete time stochastic process with countable state space $S$.*
*$X$ is called a **Markov chain**, if for all $n \in \mathbb{N}_0$ and states $i_0, \dots, i_{n-1}, i, j \in S$, the following property is fulfilled:*

$$P(X_{n+1} = j \mid X_n = i, X_{n-1} = i_{n-1}, \dots, X_0 = i_0) \;=\; P(X_{n+1} = j \mid X_n = i). \qquad (2.1)$$

The property (2.1) is called Markov property. A stochastic process fulfilling (2.1) is said to be memoryless. The state in which the process will be at the next time step only depends on the state in which the process is right now.

### 2.2 Definition
*Let $X$ be a Markov chain with state space $S$.*
*Then $t_{i,j} := P(X_{n+1} = j \mid X_n = i)$ defines the **transition probability** from state $i$ to $j$, where $i, j \in S$, $n \in \mathbb{N}_0$.*

### 2.3 Definition
*A Markov chain $X$ is called **time-homogenous**, if for all $n \in \mathbb{N}_0$ and $i, j \in S$:*

$$P(X_{n+1} = j \mid X_n = i) \;=\; P(X_n = j \mid X_{n-1} = i).$$

*This means that the probability of a transition from state $i$ to state $j$ is independent of the time step $n \in \mathbb{N}_0$.*

We assume time-homogeneity for all further Markov chains.

### 2.4 Definition
*Let $s := |S|$ be the cardinality of the state space. Further we assume a finite state space, but the concept is extendable to a countable state space and hence to infinite matrices.*
*The matrix $\mathbf{P} \in [0,1]^{s \times s}$ defined by $\mathbf{P} := \{t_{i,j}\}$, $i, j \in S$, where $t_{i,j}$ are the transition probabilities with $\sum_{j=1}^{s} t_{i,j} = 1$, is called the **transition matrix** of the Markov chain $X$.*

**2.5 Definition**
*A state $r \in S$ is called **absorbing** if for all states $s \in S \setminus \{r\}$*

$$t_{r,s} = 0.$$

*A state is called **transient** if it is not absorbing. We will denote by $T \subset S$ the set of transient states and by $R \subset S$ the set of absorbing states.*
*We call a Markov chain absorbing, if it has at least one absorbing state, $R \neq \emptyset$, and if it is possible to reach at least one absorbing state from every transient state.*

### 2.1.1 Canonical Form

The following approach for accessing absorption probabilities and times of Markov chains is described in *Grinstead and Snell* [1997, Chapter 11].
Let $X$ be an absorbing Markov chain with transition matrix $\mathbf{P} \in [0,1]^{s \times s}$. Now we rearrange the columns so that the $t$ transient states are first and the $r$ absorbing states are last, where $r + t = s$. The transition matrix now has the following canonical form:

$$\mathbf{T} := \begin{array}{|c|c|} \hline \mathbf{Q} & \mathbf{R} \\ \hline \mathbf{0} & \mathbf{I} \\ \hline \end{array} \quad ,$$

where $\mathbf{Q} \in [0,1]^{t \times t}$, $\mathbf{R} \in [0,1]^{t \times s}$, $\mathbf{I}$ is the $r \times r$-identity-matrix and $\mathbf{0}$ is the $r \times t$-zero-matrix.

**2.6 Definition**
*The matrix $\mathbf{N} \in [0,1]^{t \times t}$, defined by*

$$\mathbf{N} := \sum_{n=0}^{\infty} \mathbf{Q}^n,$$

*is called the **fundamental matrix** of the chain, where $\mathbf{Q}^0 = \mathbf{I}$ is the identity matrix.*

**2.7 Lemma: Sojourn time**
*The matrix difference $(\mathbf{I} - \mathbf{Q})$ is invertible with*

$$(\mathbf{I} - \mathbf{Q})^{-1} = \mathbf{N}$$

*and the $ij$-th entry of $\mathbf{N}$, $n_{i,j}$, is the expected number of time steps, the process will be in state $j$ before absorption, given that it starts in state $i$, for all transient states $i, j \in T$.*

A proof of lemma 2.7 can be found in *Grinstead and Snell* [1997, Chapter 11].

**2.8 Definition**
*We call $n_{i,j}$ the **expected sojourn time** in state $j$, given that the process starts in state $i$, for transient states $i, j \in T$.*

**2.9 Theorem: Absorption probability**
*Let $i \in T$ be a transient state and $j \in R$ be an absorbing state. Then the $ij$-th entry of*

$$\Phi := \mathbf{N} \cdot \mathbf{R}$$

*$\phi_{i,j}$ gives the absorption probability in state $j$ after starting in state $i$.*

Theorem 2.9 is proven in *Grinstead and Snell* [1997, Chapter 11].

**2.10 Theorem: Absorption time**
*Let $\mathbb{1}_t := (1, 1, \ldots, 1)^T \in \mathbb{R}^{t \times 1}$ be the vector of ones.*
*Then for $\tau \in \mathbb{N}^{t \times 1}$, defined by*

$$\tau := \mathbf{N} \cdot \mathbb{1}_t$$

*the i-th entry $\tau_i$ gives the expected number of time steps until absorption of the chain, after it starts in state $i$.*

**Proof:**
Lemma 2.7 showed that $n_{i,j}$ is the expected number of time steps the process will be in state $j$, given that it starts in state $i$.

Thus, summing the expected sojourn times in all transient states, $\sum\limits_{j=1}^{t} n_{i,j}$ leads to the expected number of time steps in any transient state, given the process starts in state $i$.

We see that $\tau_i = \sum\limits_{j=1}^{t} n_{i,j}$ for all $i \in T$. $\qquad\qquad\qquad\qquad\qquad\qquad\qquad\qquad\square$

## 2.2 Graph Theory

We will need some basics of graph theory to introduce a population structure on which the stochastic process occurs.

**2.11 Definition**
*Let $G := (V, E)$ define a **graph** consisting of the sets of its vertices and edges. The latter ones are also called nodes and links. If $e_{i,j} \in E$ then there is an edge going from vertex $i$ to vertex $j$, where $i, j \in V := \{1, \ldots, N\}$.*

An elegant way to represent a graph is by an adjacency matrix. Each row represents a node. The columns represent the nodes, to which that node is either connected or not.

**2.12 Definition**
*Let $\mathbf{A} \in \{0, 1\}^{N \times N}$ define the **adjacency matrix** of graph $G = (V, E)$ with nodes $i \in V = \{1, \ldots, N\}$. The $ij$-th entry of $\mathbf{A}$ is defined by*

$$a_{i,j} := \begin{cases} 1 & \text{if } e_{i,j} \in E \\ 0 & \text{if } e_{i,j} \notin E. \end{cases}$$

Although elegant in some way, the concept of adjacency matrices has a downside. For increasing number of nodes, the matrix grows quadratically with $N$. And in most cases of social, protein or neural networks, the matrix is sparse, i.e. most of its entries are zero.
With smart algorithms, sparseness can be an advantage. But otherwise the matrix just wastes a lot of memory space without providing much information.

**2.13 Remark**
   (i) In this thesis, only undirected graphs are considered – a link from $i$ to $j$ is also a link from $j$ to $i$. Therefore the adjacency matrix is symmetric, i.e. $a_{i,j} = a_{j,i}$.

(ii) We exclude self-loops – a node is not connected to itself. Thus the diagonal of the adjacency matrix is zero.

This is a question of construction. Our choice is not to let an individual replace itself. For isothermal graphs (see section 2.3.2 for a definition), this does not change the fixation probability. Even fixation time is only changed by a constant.

**2.14 Remark**

Let $G$ be an undirected graph consisting of $N$ nodes without self-loops. Then the maximum number of links is $N(N-1)$. We can see that by looking at the adjacency matrix $A$ which is an $N \times N$-matrix and therefore has $N^2$ entries.

$$
\mathbf{A} := \begin{pmatrix}
0 & 1 & 1 & \cdots & 1 & 1 \\
1 & 0 & 1 & \cdots & 1 & 1 \\
1 & 1 & 0 & \cdots & 1 & 1 \\
\vdots & \vdots & \vdots & \ddots & \vdots & \vdots \\
1 & 1 & 1 & \cdots & 0 & 1 \\
1 & 1 & 1 & \cdots & 1 & 0
\end{pmatrix}
$$

Subtracting the $N$ diagonal entries, the total number of ones in $\mathbf{A}$ is $N^2 - N = N(N-1)$.

**2.15 Definition**

*Let $G = (V, E)$ be an undirected graph. The **degree** $k_i$ of a node $i \in V$ is defined by the number of its neighbors:*

$$
k_i := |\{e_{i,j} : e_{i,j} \in E\}|.
$$

**2.16 Remark**

(i) Since the edges are binary (as opposed to weighted) here, the degree of a node $i \in V$ is equal to the sum over all incoming or outgoing edges:

$$
k_i = \sum_{j \in V} e_{i,j} = \sum_{j \in V} e_{j,i} \ .
$$

(ii) For directed graphs, one distinguishes between in-degree and out-degree. But since we restrict ourselves to undirected graphs, the degree of a node can be defined as the sum of either the outgoing or incoming edges of the node.

## 2.3   The Moran Process

To define the Moran process $M := \{M_n\}$, $n \in \mathbb{N}_0$, we first assume a well-mixed population of $N - 1$ individuals of wild type $B$ with fitness 1 into which one individual of mutant type $A$ is introduced.
The state space $S := \{0, 1, \ldots, N\}$ is defined by the number of mutants in the population. Thus, the initial state of the process is $M_0 = 1$.
We assume constant selection, i.e. the fitness of type $A$ individuals is a fixed real number $r > 0$ and does not depend on the frequency of its type. Then, one time step of the Moran process is defined by:

- One of the $N$ individuals is chosen for birth with probability proportional to its fitness.

- This individual produces a clonal offspring.

- One individual is chosen for removal uniformly at random.

- The newly produced offspring replaces the removed individual.

We assume that there are no further mutations, thus the states 0 and $N$ are absorbing.

### 2.17 Remark
This defines a simple birth-death process with exactly one birth and death per time step. By construction, the population size in this model remains constant.

For the Moran process in a well-mixed population, we obtain the following transition probabilities:

$$t_i^+ := t_{i,i+1} = P(M_{n+1} = i + 1 \mid M_n = i) = \frac{ri}{ri + N - i} \cdot \frac{N - i}{N - 1} \tag{2.2}$$

$$t_i^- := t_{i,i-1} = P(M_{n+1} = i - 1 \mid M_n = i) = \frac{N - i}{ri + N - i} \cdot \frac{i}{N - 1} \tag{2.3}$$

$$t_i^0 := t_{i,i} = P(M_{n+1} = i \mid M_n = i) = 1 - t_i^+ - t_i^- \tag{2.4}$$

where $i \in S$, $n \in \mathbb{N}_0$ and $t_i^\pm$ is the probability to increase/decrease the number of mutants by one, given that there are $i$ mutants at time $n$.
The first factor in equation (2.2) is the probability for a mutant to get chosen for birth, whereas the second factor is the probability for the death of a wild type individual. In equation (2.3), one of the wild type individuals gets chosen for birth and a mutant has to die. Equation (2.4) describes the probability of no change in the number of mutants and therefore, it is one minus the other two probabilities.
Note that we exclude self-loops and therefore the denominator in equations (2.2) and (2.3) is $N-1$ instead of the widely used $N$. An individual can not replace itself here. For the fixation probability which is defined below, this does not matter, since the quotient $\frac{t_i^-}{t_i^+} = \frac{1}{r}$ remains unchanged.

For the Moran process, the transition matrix has the following general form:

$$
\mathbf{P} =
\begin{array}{c|ccccccc}
\text{state} & 0 & 1 & 2 & \cdots & \text{N-2} & \text{N-1} & \text{N} \\
\hline
0 & t_0^0 & 0 & 0 & \cdots & 0 & 0 & 0 \\
1 & t_1^- & t_1^0 & t_1^+ & \cdots & 0 & 0 & 0 \\
2 & 0 & t_2^- & t_2^0 & \cdots & 0 & 0 & 0 \\
\vdots & \vdots & \vdots & \vdots & \cdots & \vdots & \vdots & \vdots \\
\text{N-2} & 0 & 0 & 0 & \cdots & t_{N-2}^0 & t_{N-2}^+ & 0 \\
\text{N-1} & 0 & 0 & 0 & \cdots & t_{N-1}^- & t_{N-1}^0 & t_{N-1}^+ \\
\text{N} & 0 & 0 & 0 & \cdots & 0 & 0 & t_N^0
\end{array}
$$

Since the number of mutants can only increase or decrease by one in one time step, transition matrix $\mathbf{P}$ has a tridiagonal shape.

Let us now rearrange the states, such that the transient states are first, as in section 2.1. In this case, it just means putting the first row and column to the end. Then the canonical form of the transition matrix for the Moran process is given by $\mathbf{T} \in [0, 1]^{(N+1)\times(N+1)}$ :

$$
\mathbf{T} =
\begin{array}{|c|c|}
\hline
\mathbf{Q} & \mathbf{R} \\
\hline
\mathbf{0} & \mathbf{I} \\
\hline
\end{array}
=
\begin{array}{c|ccccc|cc}
\text{state} & 1 & 2 & \cdots & \text{N-2} & \text{N-1} & \text{N} & 0 \\
\hline
1 & t_1^0 & t_1^+ & \cdots & 0 & 0 & 0 & t_1^- \\
2 & t_2^- & t_2^0 & \cdots & 0 & 0 & 0 & 0 \\
\vdots & \vdots & \vdots & \cdots & \vdots & \vdots & \vdots & \vdots \\
\text{N-2} & 0 & 0 & \cdots & t_{N-2}^0 & t_{N-2}^+ & 0 & 0 \\
\text{N-1} & 0 & 0 & \cdots & t_{N-1}^- & t_{N-1}^0 & t_{N-1}^+ & 0 \\
\hline
\text{N} & 0 & 0 & \cdots & 0 & 0 & t_N^0 & 0 \\
0 & 0 & 0 & \cdots & 0 & 0 & 0 & t_0^0
\end{array}
$$

### 2.3.1 Fixation Probability

Let $M := \{M_n\}$, $n \in \mathbb{N}_0$ be the Moran process with state space $S := \{0, 1, \dots, N\}$ and transition probabilities $t_i^+$, $t_i^-$ and $t_i^0$ for $i \in S$. However, the following result holds for general birth-death processes. The probability to get from state $i$ to the all-mutant state $N$ is given by:

$$\Phi_i^N = \frac{\sum\limits_{n=0}^{i-1} \prod\limits_{j=1}^{n} \frac{t_j^-}{t_j^+}}{\sum\limits_{n=0}^{N-1} \prod\limits_{j=1}^{n} \frac{t_j^-}{t_j^+}} \quad .$$

See *Karlin and Taylor* [1975]; *Traulsen and Hauert* [2009] for a detailed derivation.
The fixation of the mutants is impossible after their extinction (since we exclude mutations), yielding $\Phi_0^N = 0$, and the fixation is obviously certain in state $N$, therefore $\Phi_N^N = 1$.
For constant selection, that is the fitness of the types is independent of their frequency, the quotient of the transition probabilities simplifies to $\quad \frac{t_j^-}{t_j^+} = \frac{1}{r} \quad$ and therefore $\quad \prod\limits_{j=1}^{n} \frac{t_j^-}{t_j^+} = r^{-n} \quad .$

We will make use of $\quad \sum\limits_{n=0}^{i-1} r^{-n} = \frac{1-\frac{1}{r^i}}{1-\frac{1}{r}} \quad$ to obtain

$$\Phi_i^N = \frac{\frac{1-\frac{1}{r^i}}{1-\frac{1}{r}}}{\frac{1-\frac{1}{r^N}}{1-\frac{1}{r}}} = \frac{1-\frac{1}{r^i}}{1-\frac{1}{r^N}} \quad .$$

Let us denote the **fixation probability for a single mutant** by

$$\rho := \Phi_1^N = \frac{1-\frac{1}{r}}{1-\frac{1}{r^N}} \quad .$$

### 2.3.2 Isothermal Structures

Population structure can be introduced into the Moran model, see [*Lieberman et al.*, 2005; *Nowak*, 2006, Chapter 8]. Individuals of the wild type with fitness 1 inhabit the nodes of a graph. One mutant individual with fitness $r > 0$ is placed on one of the nodes at random. In most cases we will consider advantageous mutants, where $r > 1$.

At each time step, one individual gets chosen for birth with probability proportional to fitness. Then one of its neighbors dies at random to be replaced by the new offspring. Thus the links of a node determine into which neighboring sites the individual on the node can reproduce.

The standard Moran process corresponds to the complete graph, where every node is adjacent to all other nodes. Therefore, every individual in a well-mixed population has the same probability of being replaced.

**2.18 Definition**
*Let $G = (V, E)$ be an undirected graph with $N$ nodes. The **temperature** of a node is defined by the sum over all weighted incoming links:*

$$\mathcal{T}_i := \sum_{j=1}^{N} \frac{e_{j,i}}{k_j} \ ,$$

*for $i, j \in V$, $e_{i,j} \in E$ and $k_j$ being the degree of node $j$.*

A hot node has a high potential to change its state.

**2.19 Definition**
*A graph is called **isothermal**, if $\mathcal{T}_i = \mathcal{T}_j$ for all $i, j \in V$.*

Let us denote the fixation probability for the well-mixed population by $\rho_{\text{mix}} := \Phi_1^N$ which is the probability for one mutant to take over the population.

**2.20 Definition**
*A population structure represented by a graph $G$, where a mutant has fixation probability*

$$\rho_G = \rho_{mix}$$

*is called **ρ-equivalent** to the well-mixed population.*

**2.21 Theorem: Isothermal theorem**
*A graph $G$ is ρ-equivalent, iff it is isothermal.*

For a proof see *Lieberman et al.* [2005, Supplementary Notes].

### 2.3.3 Amplification and Suppression of Selection

Certain population structures increase the fixation probability of advantageous mutants compared to the well-mixed population.

**2.22 Definition**
*A graph $G$ is called **amplifier of selection**, if for $r > 1 \quad \Rightarrow \quad \rho_G > \rho_{mix}$*
*and for $r < 1 \quad \Rightarrow \quad \rho_G < \rho_{mix}$ .*


*$G$ is instead called **suppressor of selection**, if for $r > 1 \quad \Rightarrow \quad \rho_G < \rho_{mix}$*
*and for $r < 1 \quad \Rightarrow \quad \rho_G > \rho_{mix}$ .*

**2.23 Example: The star – an amplifier of selection**
Consider a graph of size $N$ with one central node and $N - 1$ leaf nodes. The latter are only connected to the center, see figure 2.1.
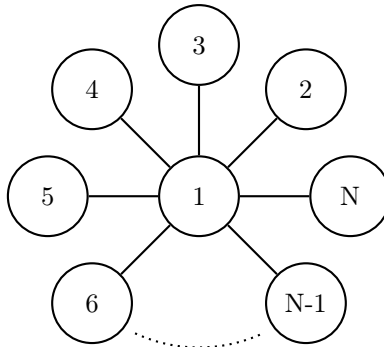


Figure 2.1: The star with $N$ nodes. All $N - 1$ leaf nodes are only connected to the center node. Note that the links are undirected here.

The adjacency matrix of the star has the following form:

$$\mathbf{A}_{\text{star}} := \begin{pmatrix} 0 & 1 & 1 & \dots & 1 \\ 1 & 0 & 0 & \dots & 0 \\ \vdots & \vdots & \vdots & \ddots & \vdots \\ 1 & 0 & 0 & \dots & 0 \\ 1 & 0 & 0 & \dots & 0 \end{pmatrix}$$

*Lieberman et al.* [2005] showed that for large $N$, the fixation probability is given by:

$$\rho_{\text{star}} = \frac{1 - \frac{1}{r^2}}{1 - \frac{1}{r^{2N}}} \ .$$

We have $\rho_{\text{star}} > \rho_{\text{mix}}$ for $r > 1$ and $\rho_{\text{star}} < \rho_{\text{mix}}$ for $r < 1$, which implies that the star is an amplifier of selection. Figure 2.3 below shows this relation for $N = 8$. Note however, that the formula for $\rho_{\text{star}}$ is only valid for large $N$. Therefore figure 2.3 only visualizes the concepts of suppression and amplification.

## 2.24 Example: The directed line – a suppressor of selection

Consider a directed line of $N$ nodes, as in figure 2.2.
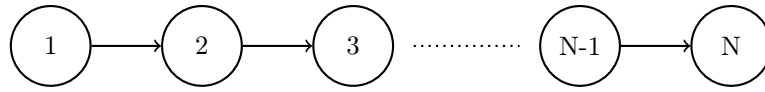


Figure 2.2: The directed line with $N$ nodes. Every individual can only reproduce into the next node.

This graph has the following adjacency matrix $\mathbf{A} \in \{0,1\}^{N \times N}$ :

$$\mathbf{A}_{\text{directedLine}} := \begin{pmatrix} 0 & 1 & 0 & \cdots & \cdots & \cdots & \cdots & 0 \\ \vdots & 0 & 1 & 0 & \cdots & \cdots & \cdots & 0 \\ \vdots & \vdots & 0 & 1 & 0 & \cdots & \cdots & 0 \\ \vdots & \vdots & \vdots & \ddots & \ddots & \ddots & & \vdots \\ \vdots & \vdots & \vdots & & \ddots & \ddots & \ddots & \vdots \\ 0 & 0 & 0 & \cdots & \cdots & 0 & 1 & 0 \\ 0 & 0 & 0 & \cdots & \cdots & 0 & 0 & 0 \end{pmatrix}$$

Note that $\mathbf{A}_{\text{directedLine}}$ is not symmetric because the graph is directed.

If the first mutant shows up at a node $i \in \{2, \ldots, N\}$, it can never take over the whole population because there is no link going back to node 1. But if it starts at node 1, it will fixate with probability 1. Thus the fixation probability is just the probability for the mutant to occur at node 1, i.e. $\rho_{\text{directedLine}} = \frac{1}{N}$ .

The line is a trivial suppressor of selection, because $\rho_{\text{directedLine}} < \rho_{\text{mix}}$ for $r > 1$ and $\rho_{\text{directedLine}} > \rho_{\text{mix}}$ for $r < 1$. The fixation probability of the directed line in comparison with the complete graph and the star is plotted in figure 2.3.
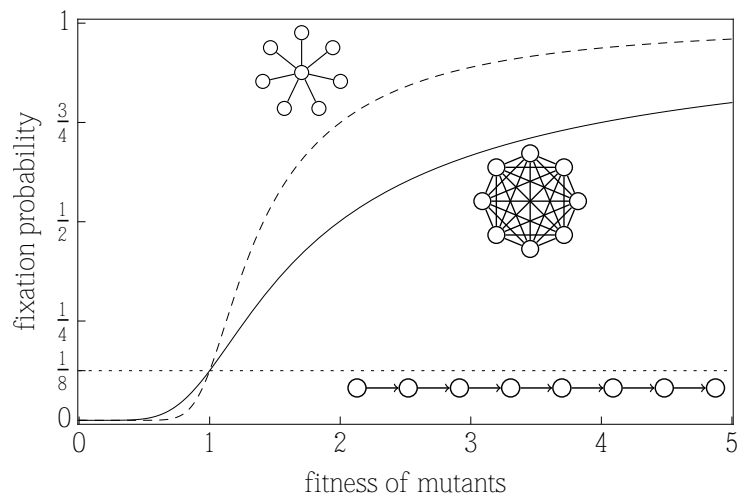


Figure 2.3: Fixation probability on three different graphs of size $N = 8$. A star (dashed), a well-mixed population (solid) and a directed line (dotted). The star graph amplifies selection compared to the well-mixed population, whereas the directed line completely suppresses selection.

### 2.3.4 Fixation Time

To measure how long the Moran process takes until absorption, we define the fixation time. We will distinguish between conditional and unconditional fixation time. Here "conditional" means: with the condition of absorption in the all-mutant state $N$. On the other hand, "unconditional" means: absorption in either one of the absorbing states $0$ or $N$.

**2.25 Definition**
*Let us call the absorption time $\tau_i$ from theorem 2.10 the expected **unconditional fixation time**, because it is not conditioned on fixing in one specific absorbing state.*

**2.26 Definition**
*For simple birth-death processes, where the states represent the number of mutants in a population, the expected **conditional fixation time** is given by:*

$$\tau_1^N = \sum_{k=1}^{N-1} \sum_{l=1}^{k} \frac{\Phi_l^N}{t_l^+} \prod_{m=l+1}^{k} \frac{t_m^-}{t_m^+} \quad , \tag{2.5}$$

[see *Karlin and Taylor*, 1975; *Traulsen and Hauert*, 2009].

**2.27 Remark**
For the well-mixed population and constant selection, the ratio of transition probabilities is given by $\frac{t_i^-}{t_i^+} = \frac{1}{r}$ for all $i \in \{1, \dots, N-1\}$.
But with the introduction of spatial population structure, the process is generally no longer a simple birth-death process. The probabilities to increase and decrease the number of mutants does not only depend on the current number of mutants, but also on their position on the graph. Therefore, the conditional fixation time on graph-structured populations is generally not given by equation (2.5).

Instead, we use a classic result to get conditional fixation times out of unconditional sojourn times [see *Ewens*, 2004; *Altrock et al.*, 2012]. For that we need the sojourn times from definition 2.8.

**2.28 Lemma: Conditional fixation time**
*Let $T$ be the set of transient states of the Moran process, $\Phi_i^N$ be the fixation probability to get from state $i$ to state $N$ and $n_{i,j}$ the sojourn time in state $j$ after starting in state $i$. Then, the conditional fixation time after starting in state $i$ is given by:*

$$\tau_i^N = \sum_{j \in T} \left( \frac{\Phi_j^N}{\Phi_i^N} \cdot n_{i,j} \right) .$$

### 2.3.5 Effective Rate of Evolution

As we have seen above, the star graph amplifies selection. As a first guess, one could try using this property for experimental evolution. In biotechnology for example, bacteria are used to produce pharmaceuticals that serve as vaccination or medication [*Moore and Arnold*, 1996; *Turner*, 2009]. A new mutant can be introduced that increases the gene expression level and therefore the resulting amount of proteins.

If the spatial position of individuals is arranged like a star (or any other amplifier of selection), the probability of success of a new advantageous mutant will increase. And since usually, the rate of evolution is considered only as $N\mu\Phi_1^N$ [*Ewens*, 2004], one might conclude that evolution is faster on stars.

Yet, this rate comes with the underlying assumption that the time it takes the successful mutant to appear is much longer, than for it to fixate. Hence, fixation time has not entered the equation so far.

But fixation time is increased on the star, as [*Frean et al.*, 2013] have shown with simulations and an approximation via separation of time scales (using the fact that the center node changes its state much faster than the leaves). To conclude, the assumption of negligible fixation time is invalid and fixation time must be included into the rate of evolution.

Therefore *Frean et al.* [2013] introduced the **effective rate of evolution** as the harmonic mean of those two rates:

$$\gamma_{\text{effect}} = \frac{1}{\frac{1}{N\cdot\mu\cdot\Phi_1^N} + \tau_1^N} \quad ,$$

where $\frac{1}{\tau_1^N}$ is the rate, at which one mutant reaches fixation.

Whenever fixation time is small compared to the rate of appearance $\tau_1^N \ll \frac{1}{N\cdot\mu\cdot\Phi_1^N}$, the effective rate of evolution reduces to the former rate of evolution.

Since this is equivalent to $\mu \ll \frac{1}{N\cdot\tau_1^N\cdot\Phi_1^N}$, the effective rate thus approximates the rate of evolution for small enough mutation rates.

If the mutation rate is large, mutants are no longer independent and two different types of mutants may be propagating through the population at the same time. We exclude that case and assume independent mutants.

However, for intermediate mutation rates, one must distinguish between graph structures. *Frean et al.* [2013] showed that for stars, the approximation fails for much smaller mutation rates than for well-mixed populations.

Since we now know the importance of fixation time, we formulate three central questions to analyze graph structures with respect to their fixation time.

**Question 1**
On every undirected graph that differs from the complete graph, is fixation time higher than in the well-mixed population?

**Question 2**
Given any population structure, does the removal of one link always lead to a higher fixation time?

**Question 3**
Does an increase in fixation probability lead to an increase in fixation time?

# 3 Small Population Size

To address question 1, whether all undirected graphs have a higher fixation time than the well-mixed population, we restrict the graph to a size of four nodes at first. Four is the smallest population size where the star graph can be distinguished from a line.

## 3.1 Graph Structure

Up to isomorphy, there are six different connected undirected graphs with four nodes. Figures 3.1 – 3.6 draw the six graph structures and their respective adjacency matrix. The number of links[1] in a graph of size four can vary between six and three. Three is the least possible number of links, where every node has at least one neighbor. When we talk about graphs hereafter, we always mean connected graphs, where no node is isolated. Disconnected graphs are not of interest in this setting, because their fixation probability is zero.

### Well-Mixed Population: Six Links

In a well-mixed population, every node is connected to every other node but itself. We will also call this structure a complete graph. On a complete graph, all nodes have the same degree, i.e. the graph is isothermal. This means for the individuals that they can reproduce into all other nodes.



$$\mathbf{A}_{\mathrm{mix}} := \begin{pmatrix} 0 & 1 & 1 & 1 \\ 1 & 0 & 1 & 1 \\ 1 & 1 & 0 & 1 \\ 1 & 1 & 1 & 0 \end{pmatrix}$$

(a)                                             (b)
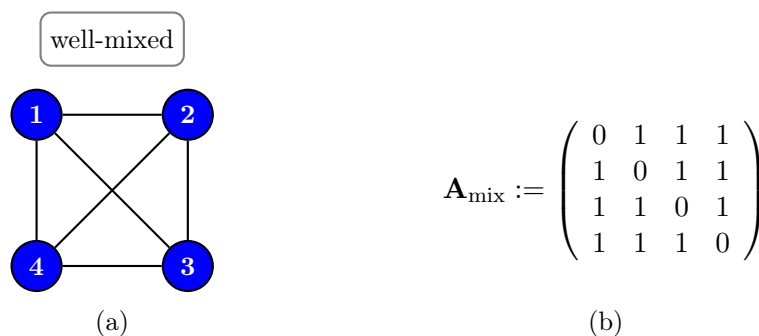
Figure 3.1: (a): Complete graph of size four with six links. This graph corresponds to the well-mixed population. (b): All entries of the adjacency matrix for a well-mixed population are one, except the diagonal, because we excluded self-loops.

---

[1]Note that the set of edges $E$ contains twice as many elements as the "number of links" to which we refer, because for one edge between $i$ and $j$ both $e_{i,j}$ and $e_{j,i}$ are elements of $E$. This inexactness is due to the use of undirected graphs. For the same reason, when we speak of a graph with six links, there are twelve ones in its adjacency matrix. This is of course redundant for symmetry reasons.

## Five Links

If we exclude one of the six links from a well-mixed population of size four, we obtain two more zeros in the adjacency matrix. The graph is visualized in figure 3.2.

Omitting the link between nodes 2 and 4 corresponds to the adjacency matrix in figure 3.2b, where the missing edges are marked in gray.



$$\mathbf{A}_{\text{fiveLinks}} = \begin{pmatrix} 0 & 1 & 1 & 1 \\ 1 & 0 & 1 & 0 \\ 1 & 1 & 0 & 1 \\ 1 & 0 & 1 & 0 \end{pmatrix}$$

(a)       (b)

Figure 3.2: (a): The graph with four nodes and five links. Note that there are two different types of nodes, those with two neighbors and those with three neighbors. (b): Adjacency matrix of the graph in (a).

## Four Links

Let us remove another link. We choose the link between the two nodes that still had three neighbors. Now every node has only two neighbors. This structure is called a ring, see figure 3.3 below. The ring is the only other isothermal structure of size four, except the complete graph.



$$\mathbf{A}_{\text{ring}} = \begin{pmatrix} 0 & 1 & 0 & 1 \\ 1 & 0 & 1 & 0 \\ 0 & 1 & 0 & 1 \\ 1 & 0 & 1 & 0 \end{pmatrix}$$

(a)       (b)
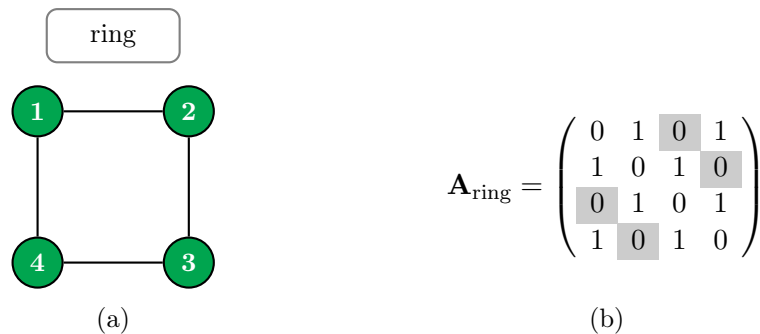
Figure 3.3: (a): Ring of size four with four links. Within the ring, all nodes are of the same type. They have a degree of two. (b): The adjacency matrix for the ring.

On the other hand, if we remove a link from a node that already had only two neighbors, we get a quite different structure, as shown in figure 3.4. Let us call it a shovel.

$$\mathbf{A}_{\text{shovel}} = \begin{pmatrix} 0 & 1 & 0 & 0 \\ 1 & 0 & 1 & 1 \\ 0 & 1 & 0 & 1 \\ 0 & 1 & 1 & 0 \end{pmatrix}$$

(a)        (b)
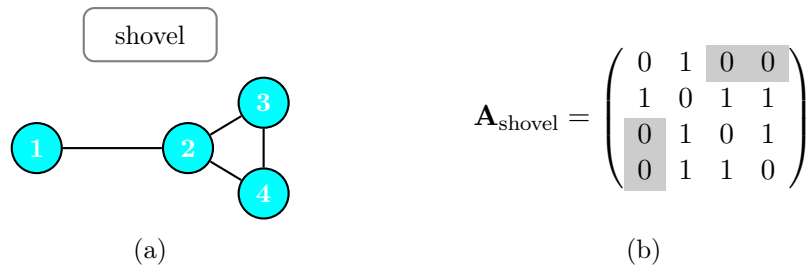
Figure 3.4: (a): Shovel with four nodes and four links. In this graph, there are three types of nodes: having either one, two or three neighbors. Node 1 is only connected to node 2, whereas nodes 2, 3 and 4 are connected to each other. (b): Adjacency matrix for the shovel. The gray marked zeros correspond to the links that are removed from a complete graph.

## Three Links

There are two distinct graphs with four nodes and three links. Those structures are called the line (see figure 3.5) and the star (see figure 3.6).



$$\mathbf{A}_{\text{line}} = \begin{pmatrix} 0 & 1 & 0 & 0 \\ 1 & 0 & 1 & 0 \\ 0 & 1 & 0 & 1 \\ 0 & 0 & 1 & 0 \end{pmatrix}$$

(a)        (b)
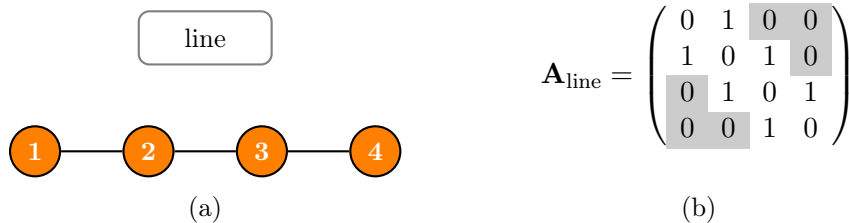
Figure 3.5: (a): Line of four nodes and three links. Note that there are two types of nodes on the line, those with one neighbor and those with two neighbors. (b): Adjacency matrix for the line.

We obtain the line by removing another link from either the ring or the shovel. The star can only be constructed by removing a link from the shovel.

Let node 1 be the center of the star, as in figure 3.6a. The center node is connected to all leaf nodes. Then the adjacency matrix is given in figure 3.6b.



$$\mathbf{A}_{\text{star}} = \begin{pmatrix} 0 & 1 & 1 & 1 \\ 1 & 0 & 0 & 0 \\ 1 & 0 & 0 & 0 \\ 1 & 0 & 0 & 0 \end{pmatrix}$$

(a)        (b)
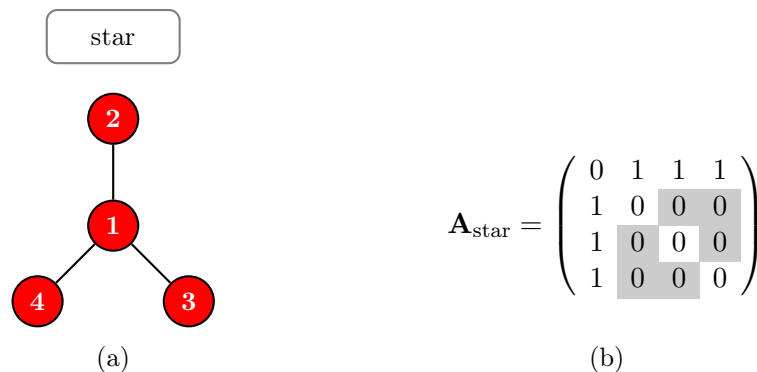
Figure 3.6: (a): Star with four nodes and three links. There are two types of nodes on the star: one node with three neighbors and three nodes with one neighbor. (b): Adjacency matrix for the star.

## 3.2 Fixation Probability

### 3.2.1 Transition Matrix

To calculate fixation probability, we first look at the different possible states and the transitions between states. Then we rearrange the states in the transition matrix like in section 2.1 so that the transient states are first.

**Six Links**

Let I, II, III and IV be the states with $1, 2, 3$ and $4$ mutants and V the state with only wild type individuals. The states of this Markov chain are shown in figure 3.7. Note that transient state numbers are highlighted in blue, whereas absorbing states are shaded in light gray.
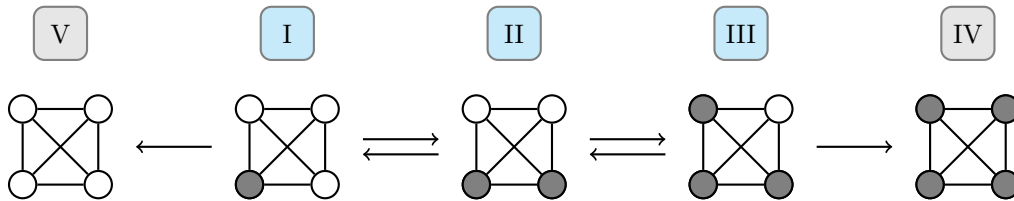


Figure 3.7: The five states of a Markov chain on a well-mixed population of size four. Gray nodes indicate mutants, whereas white nodes represent wild type individuals. The arrows show possible transitions between states of the chain in one time step. The process starts at state I and moves on the state space until it reaches one of the absorbing states IV or V.

In figure 3.7, the five different states of the Moran process on a well-mixed population of size four are displayed. State I is the initial state. If the absorbing state IV is reached, this means that the mutant achieved fixation in the population. The canonical form of the transition matrix for this process is given below. Again, transient states are highlighted in blue and absorbing states in gray.

$$
\mathbf{T}_{\mathrm{mix}} =
\begin{array}{c|ccc|cc}
\text{state} & \text{I} & \text{II} & \text{III} & \text{IV} & \text{V} \\
\hline
\text{I} & \frac{2}{r+3} & \frac{r}{r+3} & 0 & 0 & \frac{1}{r+3} \\
\text{II} & \frac{2}{3(r+1)} & \frac{1}{3} & \frac{2r}{3(r+1)} & 0 & 0 \\
\text{III} & 0 & \frac{1}{3r+1} & \frac{2r}{3r+1} & \frac{r}{3r+1} & 0 \\
\hline
\text{IV} & 0 & 0 & 0 & 1 & 0 \\
\text{V} & 0 & 0 & 0 & 0 & 1
\end{array}
\tag{3.1}
$$

The diagonal of the transition matrix $\mathbf{T}_{\mathrm{mix}}$ is positive. The Moran process stays in the same state, meaning that the number of mutants does not change, whenever a mutant replaces a mutant or a wild type individual replaces one of its kind.

With the approach given in section 2.1, we reproduce the known fixation probability of a mutant in the well-mixed population [see *Nowak*, 2006]:

$$
\rho_{\mathrm{mix}}(r) = \frac{1 - \frac{1}{r}}{1 - \frac{1}{r^4}} = \frac{r^3}{r^3 + r^2 + r + 1} \quad .
\tag{3.2}
$$

**Five Links**

Let us consider the structure with five links again. The states I,II,...,IX are shown in figure 3.8. There are several mutant-node-configurations possible in this structure, which is why the states are no longer just determined by the number of mutants on the graph. They are also determined by the degree of the respective node.
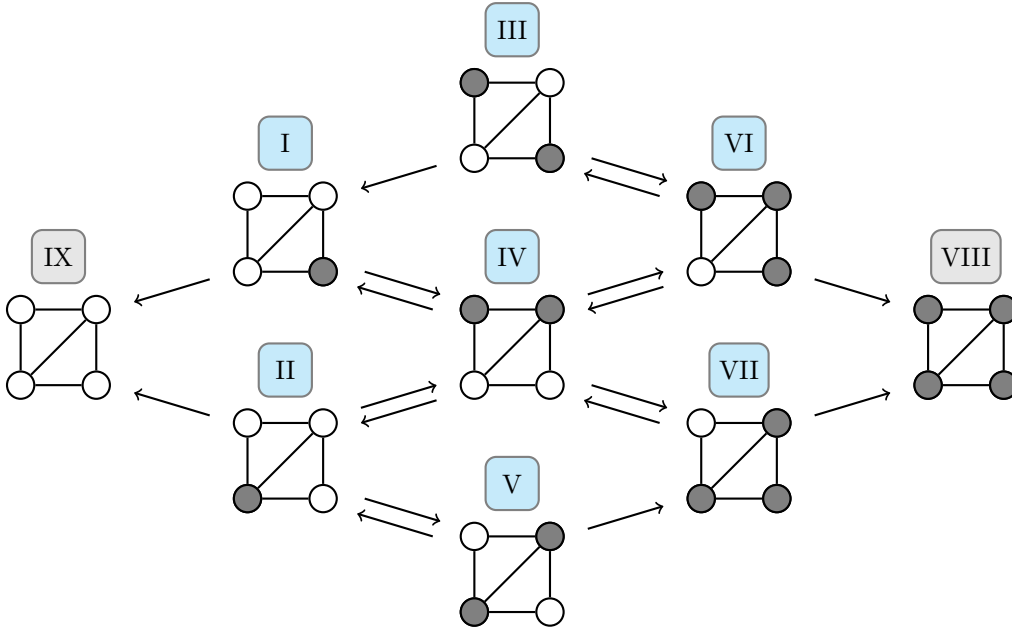


Figure 3.8: The structure with five links has four more possible states than the complete graph. There are two nodes with degree $k_i = 3$ and two nodes with degree $k_i = 2$. Therefore, one must distinguish between those two types of nodes. For example, this leads to the distinction between states I and II, which would be the same, if all nodes had the same degree. Note that even between the transient states I,II,...,VII not all transitions are bidirected. The transition probabilities $T_{\text{I,III}}$ and $T_{\text{VII,V}}$ are zero and of course, vertical transitions are not possible.

This leads to the following canonical form of the transition matrix:

$\mathbf{T} =$

| state | I | II | III | IV | V | VI | VII | VIII | IX |
|-------|---|----|----|----|---|----|-----|------|-----|
| I | $\frac{7}{3(r+3)}$ | 0 | 0 | $\frac{r}{r+3}$ | 0 | 0 | 0 | 0 | $\frac{2}{3(r+3)}$ |
| II | 0 | $\frac{2}{r+3}$ | 0 | $\frac{2r}{3(r+3)}$ | $\frac{r}{3(r+3)}$ | 0 | 0 | 0 | $\frac{1}{r+3}$ |
| III | $\frac{2}{3(r+1)}$ | 0 | $\frac{1}{3(r+1)}$ | $\frac{r}{r+1}$ | 0 | 0 | 0 | 0 | 0 |
| IV | $\frac{5}{12(r+1)}$ | $\frac{1}{4(r+1)}$ | 0 | $\frac{5r+4}{12(r+1)}$ | 0 | $\frac{r}{6(r+1)}$ | $\frac{5r}{12(r+1)}$ | 0 | 0 |
| V | 0 | $\frac{1}{r+1}$ | 0 | 0 | $\frac{r}{3(r+1)}$ | 0 | $\frac{2r}{3(r+1)}$ | 0 | 0 |
| VI | 0 | 0 | $\frac{1}{3(3r+1)}$ | $\frac{2}{3(3r+1)}$ | 0 | $\frac{5r}{3(3r+1)}$ | 0 | $\frac{4r}{3(3r+1)}$ | 0 |
| VII | 0 | 0 | 0 | $\frac{1}{3r+1}$ | 0 | 0 | $\frac{7r}{3(3r+1)}$ | $\frac{2r}{3(3r+1)}$ | 0 |
| VIII | 0 | 0 | 0 | 0 | 0 | 0 | 0 | 1 | 0 |
| IX | 0 | 0 | 0 | 0 | 0 | 0 | 0 | 0 | 1 |

The fixation probability of a single mutant on the structure with five links is given by:

$$\rho_{\text{fiveLinks}}(r) = \frac{126r^7 + 447r^6 + 643r^5 + 429r^4 + 115r^3}{126r^7 + 573r^6 + 1208r^5 + 1613r^4 + 1613r^3 + 1208r^2 + 573r + 126} \quad . \quad (3.3)$$

The strong selection limit of the fixation probability in equation (3.3) is of course $\lim_{r\to\infty} \rho_{\text{fiveLinks}}(r) = 1$.

**Four Links – Ring**

Let I, II, III and IV be the states with $1, 2, 3, 4$ mutants and V the state with no mutants, as in figure 3.9.
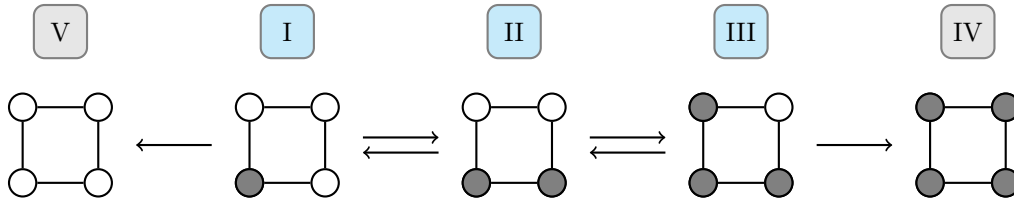


Figure 3.9: The possible states of the Moran process on the ring of size four. Note due to the special structure of the ring, mutants can only invade in a cluster, which means that there is always only one connected part of the graph inhabited by mutants.

For the ring we get the following canonical transition matrix:

$$\mathbf{T}_{\text{ring}} = \quad
\begin{array}{c|ccc|cc}
\text{state} & \text{I} & \text{II} & \text{III} & \text{IV} & \text{V} \\
\hline
\text{I} & \frac{2}{r+3} & \frac{r}{r+3} & 0 & 0 & \frac{1}{r+3} \\
\text{II} & \frac{1}{2(r+1)} & \frac{1}{2} & \frac{r}{2(r+1)} & 0 & 0 \\
\text{III} & 0 & \frac{1}{3r+1} & \frac{2r}{3r+1} & \frac{r}{3r+1} & 0 \\
\hline
\text{IV} & 0 & 0 & 0 & 1 & 0 \\
\text{V} & 0 & 0 & 0 & 0 & 1
\end{array}
\qquad (3.4)$$

Recall that the ring is isothermal. Hence, fixation probability is the same as for the well-mixed population and given by equation (3.2) as well.

### Four Links – Shovel

On the shovel, there are twelve possible states. The states and possible transitions between them are shown in figure 3.10.
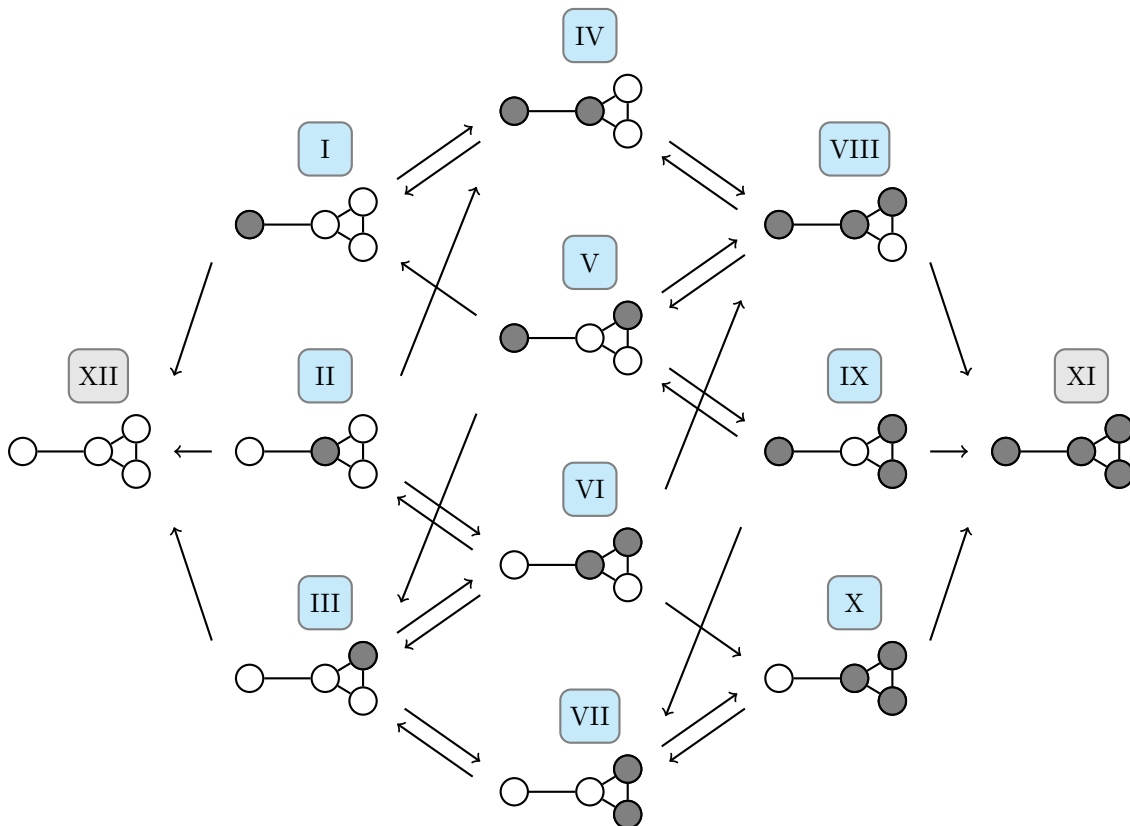


Figure 3.10: The states and transitions of the Moran process on a shovel. Note that the arrows are directed, because not all transitions are reversible. For example the process can move from state II to state IV in one time step but not back.

Since there are three types of nodes on the shovel, namely those with either one, two or three neighbors, there are three different initial states. The process starts at states I and II with probability $\frac{1}{4}$ each and at state III with probability $\frac{1}{2}$, because there are two nodes that have two neighbors.

The transition matrix for the shovel is omitted here, because it is a large $12 \times 12$-matrix. The fixation probability is a rational function with both numerator and denominator being polynomials of degree 10, therefore only the Taylor approximation for weak selection ($r \approx 1$) up to second order is provided here:

$$\rho_{\text{shovel}}(r) \approx 0.25 + 0.39(r-1) - 0.06(r-1)^2 \quad .$$

**Three Links – Line**

The line has two outer nodes with degree $k_i = 1$ and two nodes in the middle with degree $k_i = 2$. The possible states of the invasion process are shown in figure 3.11.
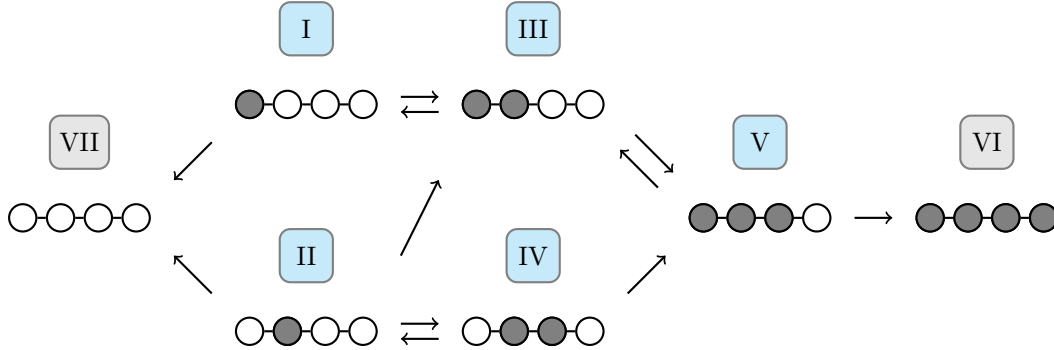


Figure 3.11: States of the Moran process on the line and all possible transitions between the states. We see that mutants can only invade in clusters. For example there is no state with just the two outer nodes occupied by mutants.

For the line, the canonical form of the transition matrix is given by:

$$\mathbf{T}_{\text{line}} = \begin{array}{c|ccccc|cc} \text{state} & \text{I} & \text{II} & \text{III} & \text{IV} & \text{V} & \text{VI} & \text{VII} \\ \hline \text{I} & \frac{5}{2(r+3)} & 0 & \frac{r}{r+3} & 0 & 0 & 0 & \frac{1}{2(r+3)} \\ \text{II} & 0 & \frac{3}{2(r+3)} & \frac{r}{2(r+3)} & \frac{r}{2(r+3)} & 0 & 0 & \frac{3}{2(r+3)} \\ \text{III} & \frac{1}{4(r+1)} & 0 & \frac{3}{4} & 0 & \frac{r}{4(r+1)} & 0 & 0 \\ \text{IV} & 0 & \frac{1}{r+1} & 0 & \frac{r}{2(r+1)} & \frac{r}{2(r+1)} & 0 & 0 \\ \text{V} & 0 & 0 & \frac{1}{3r+1} & 0 & \frac{5r}{2(3r+1)} & \frac{r}{2(3r+1)} & 0 \\ \hline \text{VI} & 0 & 0 & 0 & 0 & 0 & 1 & 0 \\ \text{VII} & 0 & 0 & 0 & 0 & 0 & 0 & 1 \end{array}$$

From this matrix, fixation probability for a mutant on the line is calculated:

$$\rho_{\text{line}}(r) = \frac{8r^5 + 16r^4 + 15r^3}{(4r^5 + 12r^4 + 19r^3 + 15r^2 + 16r + 12)2}$$

24

**Three Links – Star**

On the star, we have to distinguish between states, where the central node is inhabited by a mutant or resident. All three leaf nodes have the same graph properties. See the different states in figure 3.12.
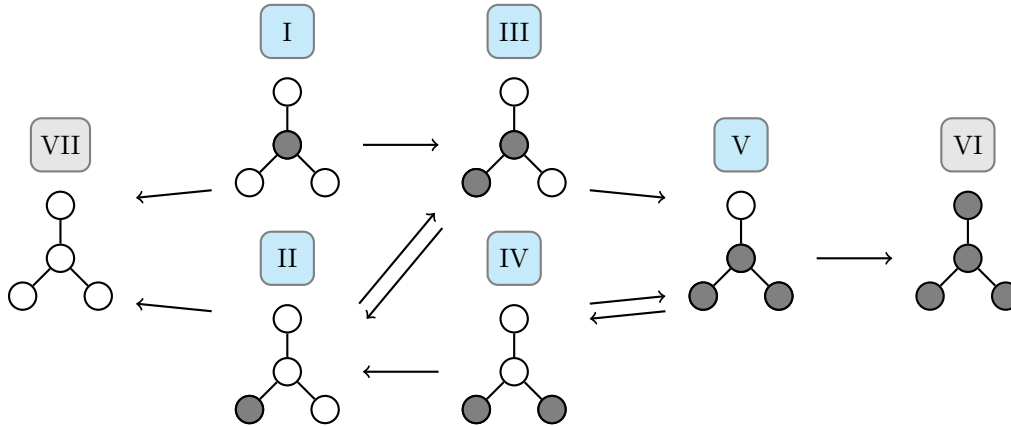


Figure 3.12: Different states of the star of size four. All possible transitions between states are indicated by directed arrows. Note that three transitions are not possible. Between the transient states, the probabilities $T_{\text{III,I}} = T_{\text{II,IV}} = T_{\text{V,III}} = 0$ are zero. It is also worthwhile mentioning, that every realization of the process starts at state I with probability $\frac{1}{4}$. Still, state I can never be reached from any other state.

Since the leaves are not connected to each other, mutants on the leaves can only place their offspring into the center node. Figure 3.6 shows, that mutant spread on the star has to occur via the center node.
The canonical form of the transition matrix for the star is:

$$
\mathbf{T}_{\text{star}} =
\begin{array}{c|ccccc|cc}
\text{state} & \text{I} & \text{II} & \text{III} & \text{IV} & \text{V} & \text{VI} & \text{VII} \\
\hline
\text{I} & 0 & 0 & \frac{r}{r+3} & 0 & 0 & 0 & \frac{3}{r+3} \\
\text{II} & 0 & \frac{8}{3(r+3)} & \frac{r}{r+3} & 0 & 0 & 0 & \frac{1}{3(r+3)} \\
\text{III} & 0 & \frac{1}{r+1} & \frac{2r}{3(r+1)} & 0 & \frac{r}{3(r+1)} & 0 & 0 \\
\text{IV} & 0 & \frac{1}{3(r+1)} & 0 & \frac{2}{3(r+1)} & \frac{r}{r+1} & 0 & 0 \\
\text{V} & 0 & 0 & 0 & \frac{1}{3r+1} & \frac{8r}{3(3r+1)} & \frac{r}{3(3r+1)} & 0 \\
\hline
\text{VI} & 0 & 0 & 0 & 0 & 0 & 1 & 0 \\
\text{VII} & 0 & 0 & 0 & 0 & 0 & 0 & 1 \\
\end{array}
$$

We see in figure 3.12, that state I cannot be reached from any other state. Therefore the first column of the transition matrix is zero.

Let us look at the fixation probability on the star and compare it to known results from the literature. The transition matrix leads to a fixation probability

$$
\rho_{\text{star}}(r) = \frac{9r^5 + 24r^4 + 7r^3}{9r^5 + 33r^4 + 28r^3 + 27r + 27} \quad . \tag{3.5}
$$

The fixation probability on the star was approximated by *Lieberman et al.* [2005] for large $N$:

$$\rho_{\text{star}}^{\textbf{Lieberman}}(r) = \frac{1 - \frac{1}{r^2}}{1 - \frac{1}{r^{2N}}} \quad .$$

(3.6)

However, since $N = 4$ is very small, we will compare our result to the formula of *Broom and Rychtář* [2008], which holds for small $N$ as well.

Let $n := N - 1$ be the number of leaf nodes, then the fixation probability on the star is given by:

$$\rho_{\text{star}}^{\textbf{Broom}}(r) = \frac{n\frac{nr}{nr+1} + \frac{r}{n+r}}{(n+1) \cdot \left(1 + \frac{n}{n+r} \sum_{j=1}^{n-1} \left(\frac{n+r}{r(nr+1)}\right)^j\right)} \quad .$$

(3.7)

For large $N$, the fixation probability in equation (3.7) reduces to the one in equation (3.6) [see *Broom and Rychtář*, 2008].

Plugging $n = 3$ into equation (3.7) leads to:

$$\rho_{\text{star}}^{\textbf{Broom}}(r)\big|_{n=3} = \frac{9r^5 + 24r^4 + 7r^3}{9r^5 + 33r^4 + 28r^3 + 27r + 27} = \rho_{\text{star}}(r) \ .$$

This showed that the method we used for calculating the fixation probability in equation (3.5) yields the same fixation probability as in *Broom and Rychtář* [2008].

### 3.2.2 Analytical and Simulated Fixation Probability

Let us look at the fixation probability on the six graph structures in figure 3.13. Analytical results from above are plotted together with simulations. We conducted $10^6$ independent realizations in C++ for fitness values $r \in \{1.5, 2, \ldots, 19.5, 20\}$.



(a)                                  (b)
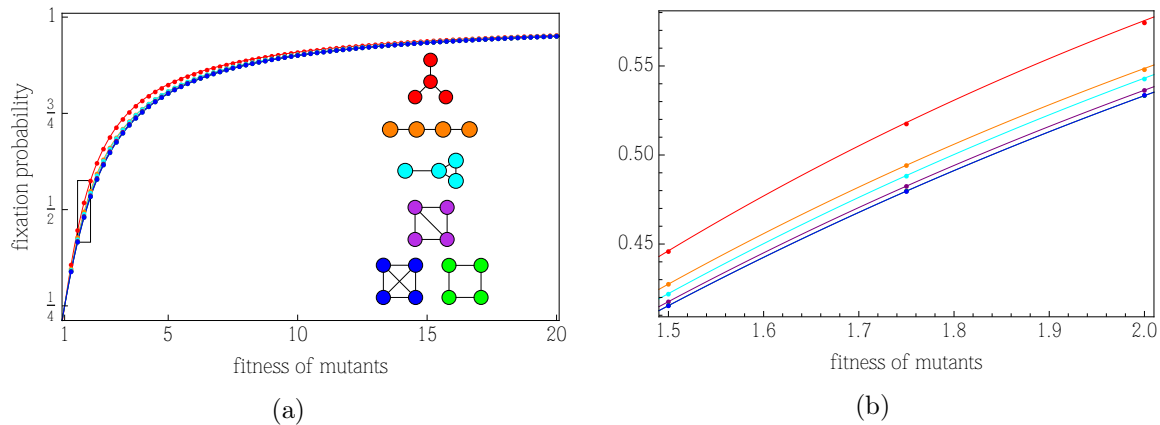
Figure 3.13: Fixation probability for six structures of size four. The graphs in the legend are drawn in the same color as the respective fixation probability. Lines show analytical results, whereas every dot represents the frequency of fixations (in state $N$) out of total number of absorptions (either in state 0 or $N$) over $10^6$ independent realizations of the process. Figure (b) shows a zoom into the black rectangle in figure (a).

The fixation probability on the six different graphs of size four is shown in figure 3.13a, which confirms concordance of simulations with analytical results.

It can be seen, that the star increases fixation probability for advantageous mutants. To have a closer look, the area where mutants' fitness is between $1.5 < r > 2$, is enlarged in figure 3.13b. This shows that the structure with five links, the shovel, the line and the star are amplifiers of selection, whereas the ring is $\rho$-equivalent to the well-mixed population.

## 3.3 Fixation Time

The last section showed that all structures of size four except the ring are amplifiers of selection. To answer question 3, whether amplification of selection leads to an increase in fixation time, this section analyzes fixation time.

### Complete Graph

We calculate the fixation time as described in section 2.1 with Mathematica. The mean conditional fixation time for the well-mixed population depending on the fitness $r > 0$ of the mutants is:

$$\tau_{\text{mix}}(r) = \frac{11r^2 + 14r + 11}{2r^2 + 2} \ ,$$

for weak selection ($r \approx 1$), this can be approximated by the following Taylor approximation up to second order:

$$\tau_{\text{mix}}(r) \ \approx \ 9 \ - \ \frac{7}{4}(r-1)^2 \ . \tag{3.8}$$

The Taylor approximation in equation (3.8) shows that the fixation time has a vanishing linear term. The fixation time has its maximum at $r = 1$. Both advantageous and disadvantageous mutants have a lower fixation time, because of the negative quadratic term.

### Five Links

The fixation time $\tau_{\text{fiveLinks}}(r)$ is a rational function with both numerator and denominator of degree 15 with up to 13-digit coefficients. Therefore, only the Taylor approximation for weak selection up to second order is included here:

$$\tau_{\text{fiveLinks}}(r) \ \approx \ 10.7 \ + \ 0.4(r-1) \ - \ 2.5(r-1)^2 \ . \tag{3.9}$$

It can be seen in equation (3.9), that the Taylor expansion of fixation time also includes a linear term, as opposed to the one for the well-mixed population in equation (3.8). This means that slightly advantageous mutants invade slower than neutral ones. But intermediately and highly advantageous mutants, as well as disadvantageous mutants, decrease fixation time, because of the negative quadratic term.

### Ring

From the transition matrix, the expected conditional fixation time on the ring is calculated:

$$\tau_{\text{ring}}(r) = \frac{6r^2 + 8r + 6}{r^2 + 1} \ ,$$

with a weak selection Taylor approximation of:

$$\tau_{\text{ring}}(r) \approx 10 - 2(r-1)^2 \quad . \tag{3.10}$$

The Taylor series of fixation time on the ring, as given by equation (3.10) above, has no linear term, but has a maximum at $r = 1$, like the Taylor expansion of fixation time on the complete graph in equation (3.8). Therefore advantageous and disadvantageous mutants fixate faster than neutral mutants.

### Shovel

Since the fixation time $\tau_{\text{shovel}}(r)$ on the shovel is a huge rational function, where both numerator and denominator are of degree 31 with up to 25-digit coefficients, we omit it here. The Taylor approximation for weak selection ($r \approx 1$) up to second order is given by:

$$\tau_{\text{shovel}}(r) \approx 16 + 0.7(r-1) - 4(r-1)^2 . \tag{3.11}$$

The approximation in equation (3.11) contains a linear term like the approximation for the structure with five links in equation (3.9). Therefore, mean fixation time is not maximal at $r = 1$, but mildly advantageous mutants have an increased fixation time on the shovel. Again, intermediately and highly advantageous, as well as all disadvantageous mutants, fixate faster than neutral ones.

### Line

On the line, fixation time dependent on mutants' fitness is given by:

$$\tau_{\text{line}}(r) = \frac{168r^6 + 864r^5 + 2160r^4 + 3119r^3 + 2820r^2 + 1431r + 306}{16r^6 + 56r^5 + 104r^4 + 106r^3 + 105r^2 + 84r + 36} ,$$

Let us look at the Taylor approximation for weak selection:

$$\tau_{\text{line}}(r) \approx 21.3 + 0.6(r-1) - 8(r-1)^2 . \tag{3.12}$$

The maximum of the approximated mean fixation time in equation (3.12) is shifted to slightly beneficial mutants like in equations (3.9) and (3.11).

### Star

The expected conditional fixation time on the star is given by:

$$\tau_{\text{star}}(r) = \frac{351r^5 + 729r^4 + 1098r^3 + 910r^2 + 543r + 81}{27r^5 + 27r^4 + 36r^3 + 28r^2 + 33r + 9} ,$$

with a weak selection approximation:

$$\tau_{\text{star}}(r) \approx 23.2 + \frac{3}{4}(r-1) - 8.9(r-1)^2 . \tag{3.13}$$

Equation (3.13) shows that neutral mutants have the highest fixation time on the star, compared to neutral mutants on the previous five graph structures, because the constant term is larger than that of all previous structures. But again, slightly advantageous mutants fixate slower than neutral ones.

To summarize the analytical results of this section, the following table gives an overview of mean fixation time for all six graphs of size four. Since those six functions do not intersect in the interval $r \in [1, \infty]$, only the two limiting cases, which are neutral and strong selection, are included here.

Table 3.1: Different graphs of size four with their respective mean fixation time at $r = 1$ and their strong selection limit of the mean fixation time.

| Graph structure | $\tau_{\text{structure}}(r)\big|_{r=1}$ neutral selection | $\lim\limits_{r \to \infty} \tau_{\text{structure}}(r)$ strong selection |
|---|---|---|
| Star | 23.2 | 13 |
| Line | 21.3 | 10.5 |
| Shovel | 16 | 9.8 |
| Five links | 10.7 | 6.5 |
| Ring | 10 | 6 |
| Complete graph | 9 | 5.5 |

In table 3.1 we compare the mean fixation time of the different graph structures for neutral mutants with fitness $r = 1$ and very advantageous mutants with fitness $r \to \infty$.

For the six structures that were discussed in this section, we saw that only the isothermal structures (complete graph and ring) have a maximum mean fixation time at $r = 1$. On the other four structures, slightly advantageous mutants fixate slower than neutral mutants.

### 3.3.1 Visualization of the Analytical Results for Fixation Time

The results for the six different graph structures with four nodes are visualized in figure 3.14. The mean conditional fixation time $\tau$ is plotted as a function of the mutant's fitness $r$. As anticipated, the star shows a higher fixation time than the well-mixed population.
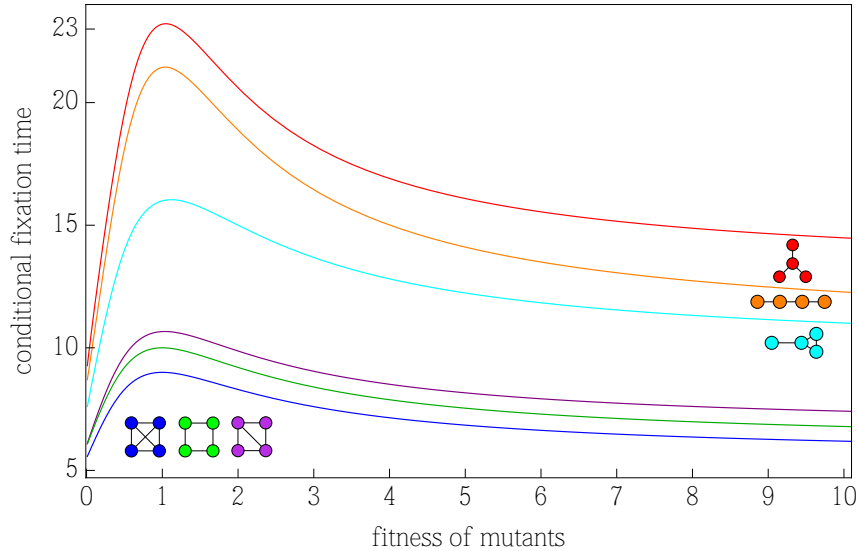


Figure 3.14: The mean conditional fixation time on the six different population structures of size four. Numbers in brackets indicate how many links the respective graph has.

In figure 3.14 we can see that the removal of one link leads to a higher fixation time than on the complete graph. However, if another link is omitted (ring), the fixation time goes down again! This result is very surprising and non-intuitive. Question 2, whether in any given graph, the removal of one links increases fixation time, can not be proven, since we hereby found a counter example.
The shovel has four links as well, but increases the fixation time compared to the structure with five links.
Also note that the star shows a higher fixation time than the line, even though they both have three links. This is very interesting since it shows that fixation time is in general neither determined by the number of links nor equivalently by the average degree of a node.

Table 3.2: Different graphs of size four and their respective number of links and average node degree. The structures are ordered according to decreasing fixation time.

| Graph structure | Number of links | Average node degree |
|---|---|---|
| Star | 3 | 1.5 |
| Line | 3 | 1.5 |
| Shovel | 4 | 2 |
| Five links | 5 | 2.5 |
| Ring | 4 | 2 |
| Full graph | 6 | 3 |

Table 3.2 further illustrates this issue. For each graph structure, the table displays the corresponding number of links and the average node degree. Since the structures are ordered according to decreasing fixation time, we observe that there is no monotonous pattern in the number of links. The fixation time of the structure with five links is in between that of the shovel and the ring, but it has five links, as opposed to the other's four links. There is no monotonicity in the average node degree either, because the second column of table 3.2 can be calculated from the first.

### 3.3.2 Simulation of Fixation Time

Let us compare the analytical results from the last section to simulations. For the fitness $r$ of type $A$, the values $r \in \{1.5, 2, \ldots, 19.5, 20\}$ are used to perform $10^6$ independent realizations, using C++. Figure 3.15 shows the average fixation time of one advantageous mutant in a population of size four. The analytical result is plotted together with the simulations.
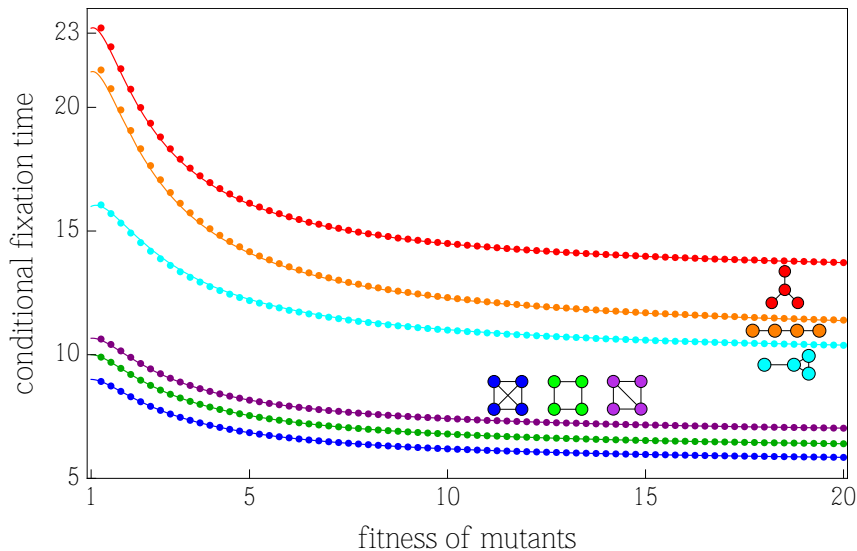


Figure 3.15: The average conditional fixation time on the six population structures of size four. Lines represent the analytical result and dots are simulations.

Figure 3.15 shows that on all graphs of size four, fixation time is higher than on the complete graph. On the ring, the increase is approximately one time step, whereas the structure with five links increases fixation time a little more. The structures shovel, line and star have a much higher fixation time.

These results answer question 1 for population size four. On every structure of size four that differs from the complete graph, fixation time is increased.

During this section, we found a counter example that answers question 2 negatively. The removal of one link apparently does not always prolong the process of absorption. In figure 3.15 we see that although the ring is constructed by dropping one link from the structure with five links, fixation is faster on the ring than on the structure with five links. This result is counterintuitive and needs a closer investigation, which will follow in chapter 4.2.

## 3.4   Sojourn Time

In this section, the expected sojourn times (see definition 2.8) in all transient states of each structure of size four are analyzed for a better understanding of the conditional fixation time.

During the remainder of this section, states with one mutant are plotted in red, two-mutant states are blue and states with three mutants are green. Lines in the figures represent analytical results and the dots are averaged over one million independent realizations.

Note that the sum over all sojourn times is just the unconditional fixation time, because this yields the overall time which the process spends in any state before absorption.

### Complete Graph and Ring

For the isothermal ring and well-mixed population, the sojourn times are plotted in figure 3.16.



(a) complete graph                 (b) ring
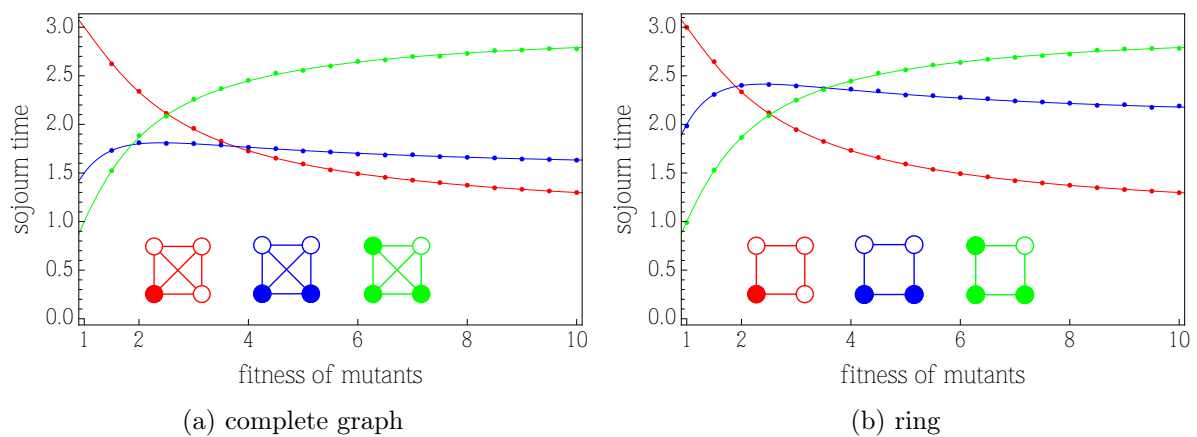
Figure 3.16: (a): The sojourn time in the three transient states of a complete graph of size four depending on the fitness of the mutants. For neutral evolution ($r = 1$), the sum of the sojourn times is 5.5, which is the unconditional fixation time. Figure (b) shows the sojourn times in the states of the ring. For weak selection, the process spends the most time in state I and the fewest in state III. For strong selection, the probability of mutant invasion increases, and therefore, the process visits state III more often.

For slightly advantageous mutants, the process stays in state I the longest. With increasing fitness of the mutants, sojourn in state III gets longer. This holds for both the complete graph and the ring.

It can be seen in figure 3.16, why the ring has a higher fixation time than the well-mixed population. The sojourn time in states I and III is exactly the same as in the well-mixed population. But on the ring, the process stays in state II for a longer time.

On the ring, unconditional fixation time for neutral evolution is 6, which is half a time step more than on the complete graph.

## Five Links

It was shown in subsection 3.3.1, that the structure with five links increases fixation time compared to the well-mixed population. Now the sojourn times are displayed in figure 3.17.
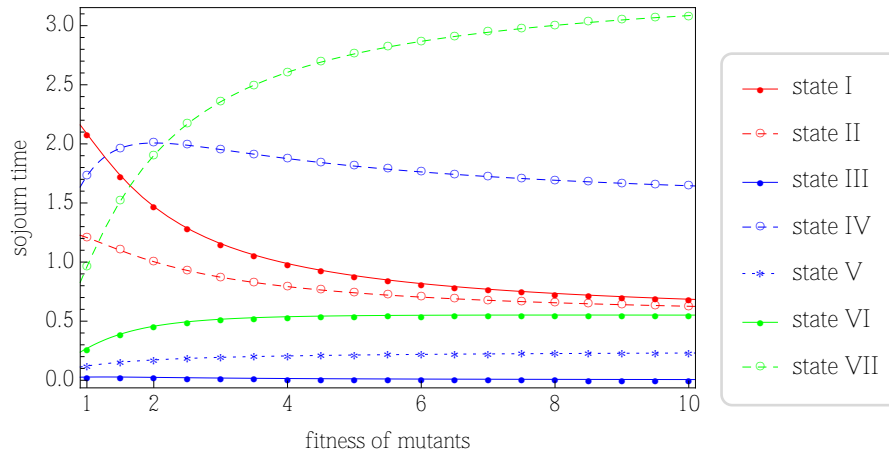


Figure 3.17: The sojourn time at the seven transient states of the structure with four nodes and five links.

The states I and VII are symmetric regarding their properties in the state space. They both have two incoming transitions and two outgoing transition (see figure 3.8). On the other hand, states II and VI have two incoming but three outgoing transitions. This is reflected in the sojourn times in figure 3.17 as well, namely in the way that the process stays in states I and VII for a long time. State IV is also visited a lot, because it has four incoming and outgoing links. For weak selection, the process stays the longest in state I. For strong selection, state VII shows the highest sojourn time.
State III is almost never visited, independent of selection intensity. The sojourn in state V is short as well, because from state II it is twice as likely to move to state IV, as to state V. Additionally, state V has no incoming link from the states with three mutants.
We observe that for strong selection, sojourn time in the one-mutant-states I and II is approximately the same.

**Four Links: Shovel**

For the shovel, sojourn times in all transient states are plotted in figure 3.18.
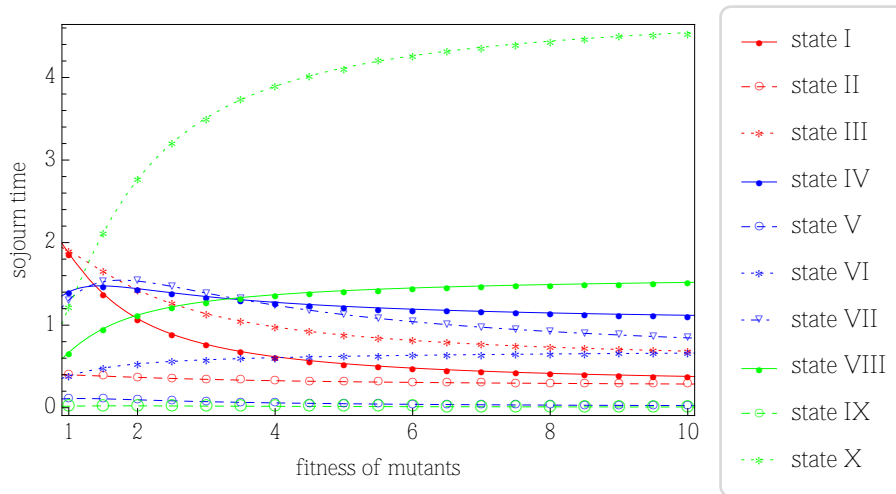


Figure 3.18: Sojourn times on the shovel

By looking at figure 3.10 again, we see that there is no direct path from a one-mutant-state through states V and IX. Therefore, it is clear that the sojourn time in states V and IX is almost zero. Also, state II has only one incoming link and thus a very low sojourn time.

Most of the paths go through state X with a high probability, therefore the process shows the highest sojourn time in state X in figure 3.18.

**Three Links: Line**

Sojourn times on the line are shown in figure 3.19.
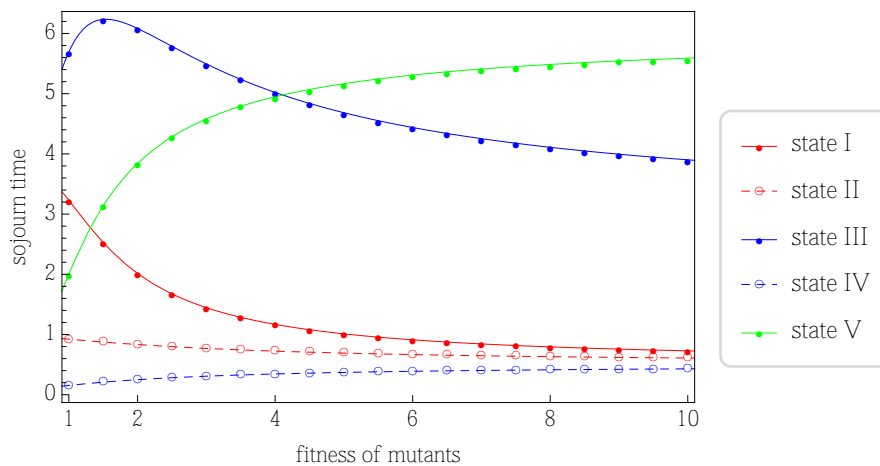


Figure 3.19: Sojourn times on the line.

For weak selection, the process stays longest in state III (see figure 3.11) with a single mutant at one of the inner nodes. This changes for strong selection, where state V with three mutants

has the highest sojourn time.

Already for weak selection, sojourn time in state III is much higher than in state I.

## Three Links: Star

The star showed the highest conditional fixation time in subsection 3.3.1. Let us analyze the sojourn time in the transient states of the star in figure 3.20.
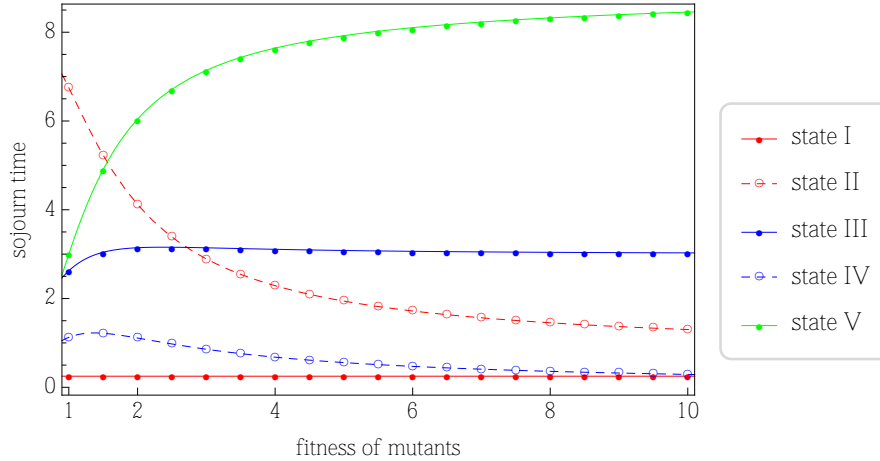


Figure 3.20: Sojourn times on the star of size four.

In figure 3.20, sojourn time in state I is almost zero. State I has one mutant at the center node, therefore there is no other state with a possible transition to state I. State IV is rarely visited as well, because none of the one-mutant-states are connected to it.

Already for intermediate selection strength, sojourn time in state V is very long, which leads to a high fixation time.

Comparing the structures of size four, we see that they all have a similar green curve (sojourn in a state with three mutants) in common. The values are different, but the shape is very similar.

## 3.5 Effective Rate of Evolution

Using the fixation probability and time that were calculated in the previous sections, we now focus on the effective rate of evolution. Recall that the effective rate of evolution, which was introduced by *Frean et al.* [2013], is given in chapter 2.3.5 by:

$$\gamma_{\text{effect}} = \frac{1}{\frac{1}{N \cdot \mu \cdot \Phi_1^N} + \tau_1^N} \quad ,$$

where $N$ is the population size, $\mu$ is the mutation rate, $\Phi_1^N$ is the fixation probability and $\tau_1^N$ is the fixation time of one single mutant.

Figure 3.21 visualizes the effective rate of evolution on all six graphs of size four as a function of mutation rate with fixed mutant fitness $r = 2$. Small mutation rates, where $\mu \in \left[10^{-4}, 10^{-3}\right]$, are used in figure 3.21a, whereas figure 3.21b plots effective rates against intermediate mutation rates, $\mu \in \left[10^{-2}, 3 \cdot 10^{-2}\right]$.
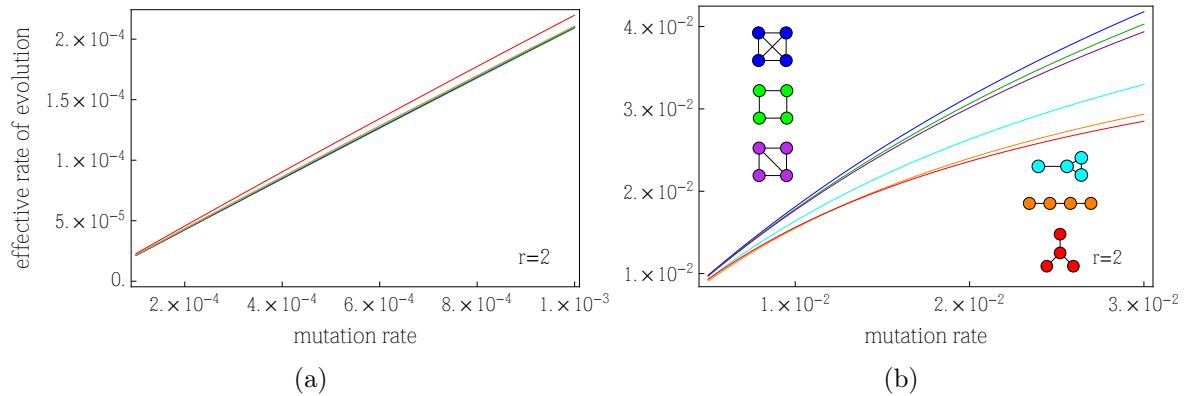


Figure 3.21: Effective rate of evolution on all six graph structures of size $N = 4$ plotted against (a): very small mutation rates and (b): intermediate mutation rates. The mutants' fitness is fixed at $r = 2$ in both figures.

The star shows the highest effective rate of evolution in figure 3.21a, compared to the other five graphs of size four. This is due to the fact that for small mutation rates, the effective rate of evolution is mainly determined by fixation probability. And since the star has the highest fixation probability, evolution proceeds fastest on the star for small mutation rates.

In figure 3.21b on the other hand, the effective rate of evolution sorts the six graphs according to the inverse order of fixation time. There, the effective rate of evolution is highest on the complete graph. For intermediate mutation rates, the effective rate of evolution is most influenced by fixation time. Otherwise, the isothermal ring would not be slower than the complete graph.

To find out at which mutation rate the switch between the importance of fixation probability and fixation time happens, we look at the two most distinct cases – the complete graph and the star.
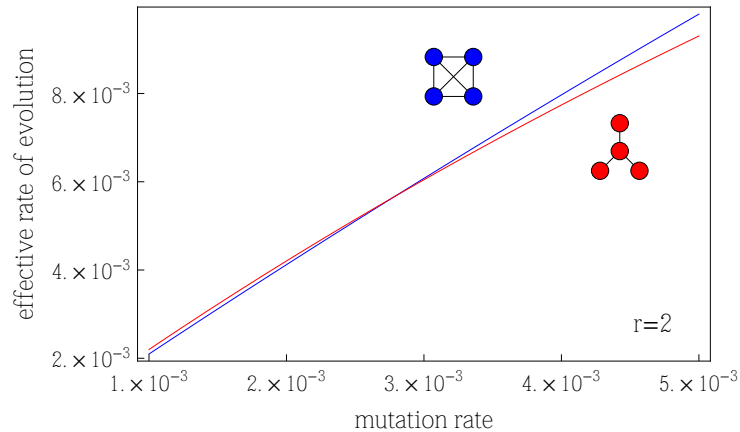


Figure 3.22: Effective rate of evolution on the star and the well-mixed population. Note that mutants' fitness is fixed at $r = 2$ again.

Figure 3.22 shows that at a mutation rate around $\mu \approx 3 \cdot 10^{-3}$, the effective rate of evolution on the star and on the well-mixed population intersect. For smaller mutation rates, evolution proceeds faster on the star than on the well-mixed population, whereas this relation is reversed for larger mutation rates.

39

## 3.6   Location of the First Mutant

So far, the first mutant was introduced at a random node at the beginning of every realization of the process. Conditional fixation time was calculated as the average over a certain number of these realizations.

The aim of this section is to investigate the effect of initial mutant placement on fixation time. Does it prolong fixation time if the first mutant is put on a node with fewer neighbors? We will not analyze the complete graph and the ring in this section, because all of their nodes have the same number of links. This means that there is only one possible initial condition for each of them.

### Five Links

The graph with four nodes and five links has two types of nodes, namely with either two or three neighbors. We place the first mutant randomly at one of the four nodes and plot fixation time for the two types of nodes in figure 3.23.
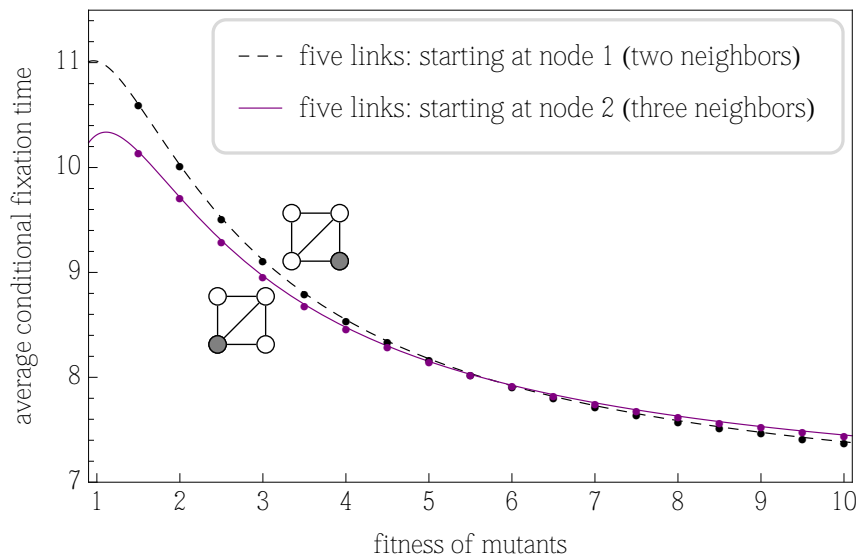


Figure 3.23: The average conditional fixation time on the structure with four nodes and five links. The first mutant starts either at node 1 (dashed black line) which has two neighbors or at node 2 (purple line) which has three neighbors. Dots represent the simulated average over $10^7$ independent realizations.

In figure 3.23, we see that the initial position of the mutant has an impact on fixation time. For small values of $r$, fixation when starting at node 1 takes longer than fixation when starting at node 2. This changes around $r \approx 5.8$. For larger values of $r$, starting at node 2 leads to a slightly higher fixation time than starting at node 1.

**Shovel**

Let us investigate fixation time on the shovel. In figure 3.24, three different types of nodes are distinguished – such with either one, two or three neighbors. The process is started at those three different nodes and the respective fixation times are plotted.
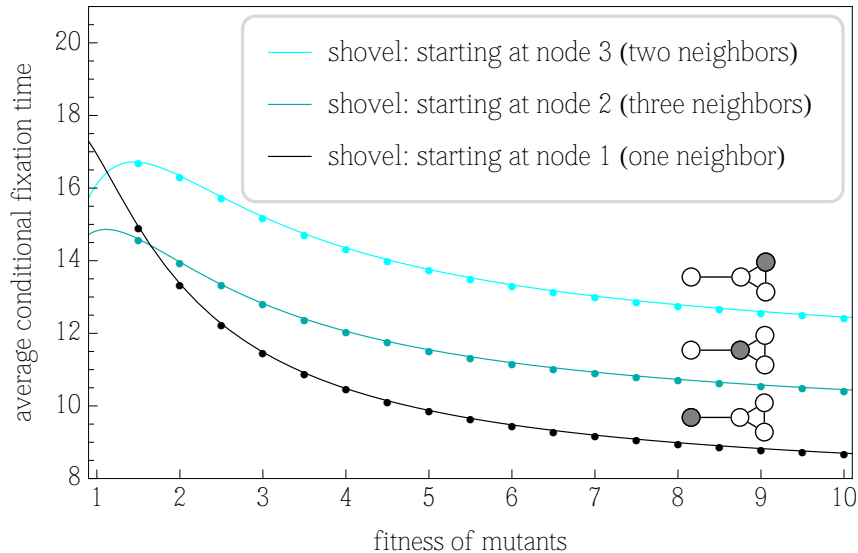


Figure 3.24: Average conditional fixation time simulated (dots) and computed (lines) on the shovel. The mutant has three different possibilities to start at either node 1 (black line), node 2 (dark turquoise line) or node 3 (cyan line). The latter is equivalent to starting at node 4. The simulations are conducted by starting the process at the three different nodes of interest. Then the fixation time for each of them is averaged over those $10^7$ independent realizations of the process.

For mutants with a small fitness advantage, there is a monotonicity in the fixation time depending on the node degree. The fewer neighbors one node has, the higher the fixation time.

But for most values of $r$, the fixation time is highest when starting from node 3. This result is surprising, because node 3 has two neighbors and therefore more neighbors than node 1, which shows a lower fixation time.

Interestingly, there are two intersections of the black curve with the other two curves for mutant fitness between $1 < r < 2$, meaning that the preferential starting node changes depending on the fitness.

Apparently, a mutant on the shovel should start at node 1 for most fitness values..

## Line

On the line, fixation time is the same when starting at node 1 or 4 because they both only have one neighbor. Similarly, starting at nodes 2 or 3, which both have two neighbors, shows the same fixation time. Due to this redundancy, we only need to include two different initial conditions into our analysis.
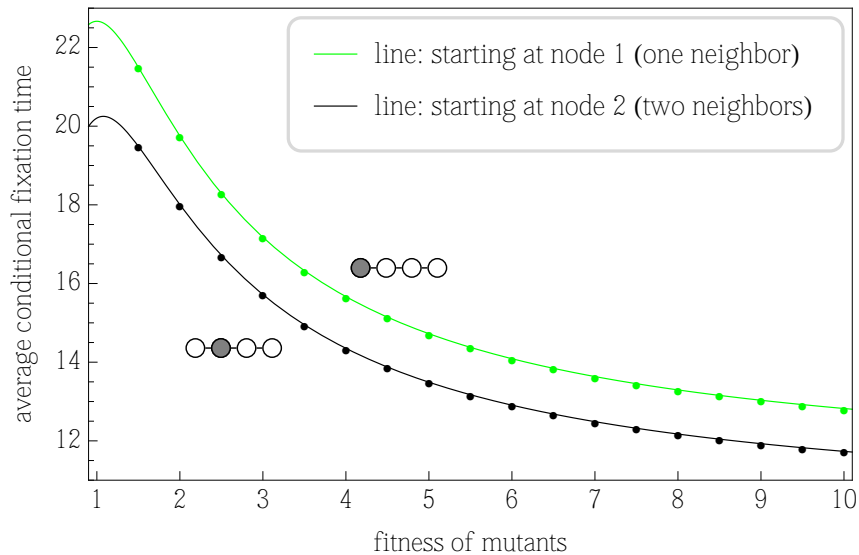


Figure 3.25: Fixation time on the line plotted against the fitness of mutants. Again, lines represent analytical results, whereas dots represent simulations. The time to fixation after starting at node 1 is given in green. The time after starting at node 2 is represented by the black line.

In figure 3.25, we see that starting at node 1 increases fixation time, compared to node 2 for all plotted values of mutant fitness $r$. Indeed, it is intuitively accessible that a mutant at an outer node of the line takes longer to fixate than at an inner node.

**Star**

Let us look at different initial conditions for the Moran process on the star-structured population of size four. In this analysis, we only need to distinguish between the center and leaf nodes, because all leaf nodes share the same graph properties.
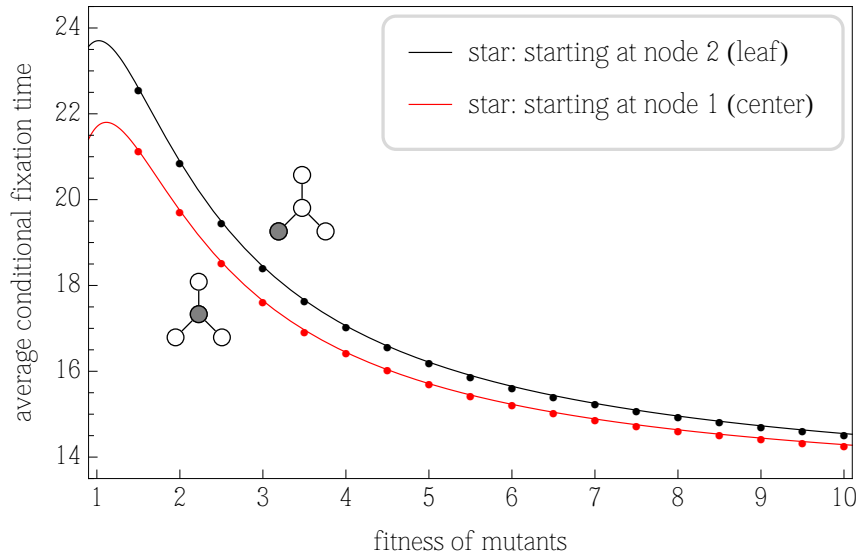


Figure 3.26: The average conditional fixation time simulated (dots) and computed (lines) on the star. The mutant starts at the center node (red) and at one of the leaf nodes (black).

In figure 3.26, fixation time is shorter when starting at the center node. As expected, a mutant starting at a more isolated leaf node takes longer to fixate.

Note that the difference between the two initial conditions is smaller on the star than on the line. This can be explained by the fact that a mutant at a leaf node has to proceed via the center. And a mutant at the center node only reproduces into a leaf. Therefore, the processes that started at either of the two initial nodes are essentially identical after the birth of the second mutant. But the process which starts at a leaf lags behind, because that specific leaf node has to be chosen for birth, before it can propagate through the center node. The difference grows ever smaller for increasing fitness of the mutants. Because with increasing fitness, the probability to choose the mutant at the leaf node tends to one, which makes the two processes almost identical (on average).

This section indicates that the shortest average fixation time does in fact depend on the position of the first mutant. While small on the structure with five links, the effect is more prominent in the remaining three structures.

# 4  Larger Graphs

In this chapter, we investigate the effect of population structure on fixation time for larger graphs. At first, simulations are conducted for population size $N = 8$. Then we focus on the effect which we have seen in section 3.3.2, where the structure with five links had a higher fixation time than the ring with four links. We increase the population size to check whether this effect is still present.

## 4.1  Size Eight

We simulate $10^6$ independent realizations of a Moran process on different population structures with eight individuals.
For the mutant's fitness $r$, the values $r \in \{1.25, 1.5, \dots, 9.75, 10\}$ are used. Even though only the simulations for graph size $N = 8$ are shown, the results for size $N = 16$ are qualitatively similar.
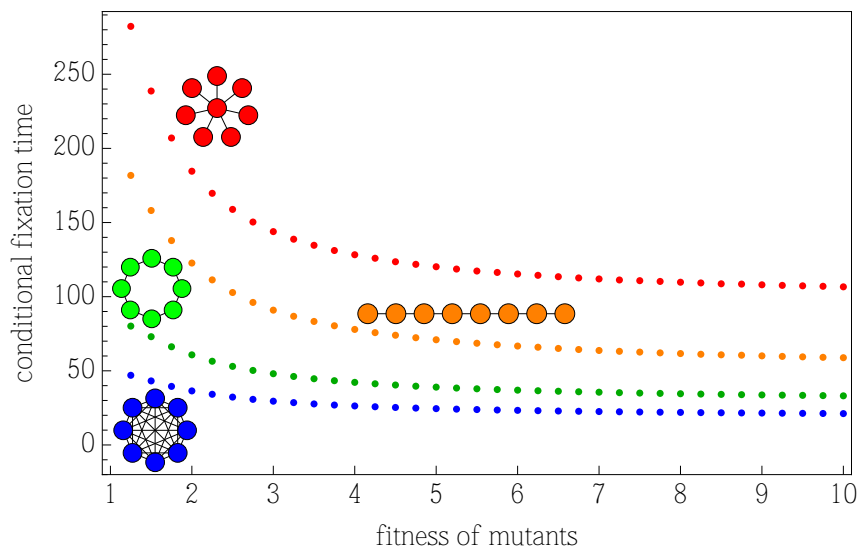


Figure 4.1: Simulated fixation time on four different population structures of size $N = 8$. The complete graph (blue) consists of 28 links. The ring (green) has 8 links, whereas the line (orange) and star (red) both have only 7 links, which is the minimal number of links in a connected graph of size 8.

In figure 4.1, we see that the ring with 8 links increases fixation time. As expected, the line and star, which both have 7 links, increase it substantially more. But at this scale, there is no visible

difference between the fixation time for the structures with 26 and 27 links and the well-mixed population. Therefore those structures are plotted again in figure 4.2 to have a closer look.

### 4.1.1 Removal of One and Two Links

Fixation time for graphs with 8 nodes and 26 or 27 nodes is compared to fixation time in the well-mixed population in figure 4.2.
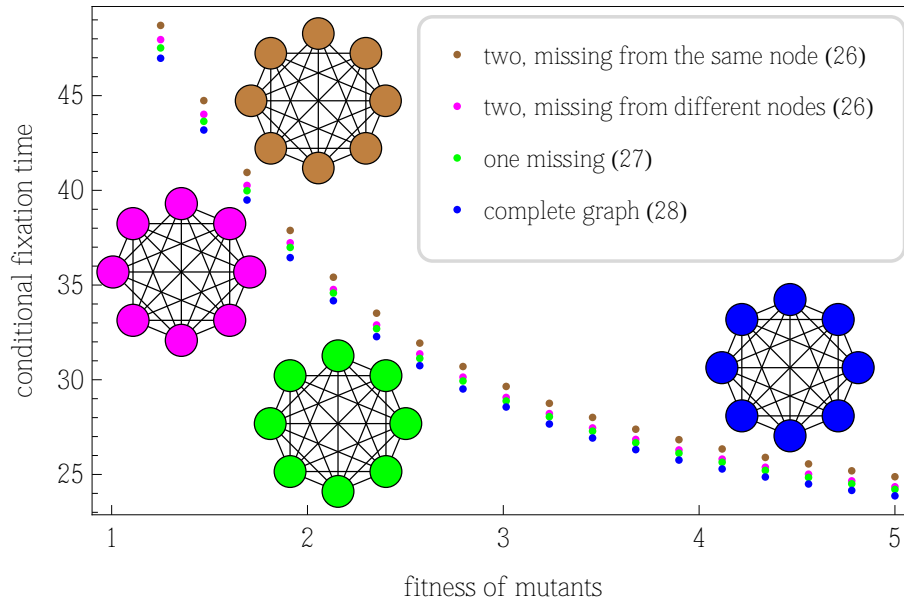


Figure 4.2: Closer look at the fixation time on the structures, that show very little difference from the complete graph. Numbers in brackets indicate the total number of links in the respective graphs. The graphs in the legend are drawn in the same color as their fixation time.

In figure 4.2, the fixation time on the complete graph and on the complete graph minus one and two links is plotted against the fitness of the mutants. The structure, where two links are omitted from the same node (brown, 26 links), shows the highest fixation time. The graph which has two links missing from different nodes (magenta, 26 links) has a higher fixation time than the structure with 27 links (green) and the well-mixed population (blue, 28 links).
However, the differences are very small, because only one or two out of 28 links are missing.

### 4.1.2   Removal of Three Links

Next, let us remove three links from the complete graph. There are five different ways to omit three links in a graph of size eight. We analyze the fixation time in these five structures with eight nodes and 25 links. This is visualized in figure 4.3a.
The respective graph structures are indicated in figure 4.3b.
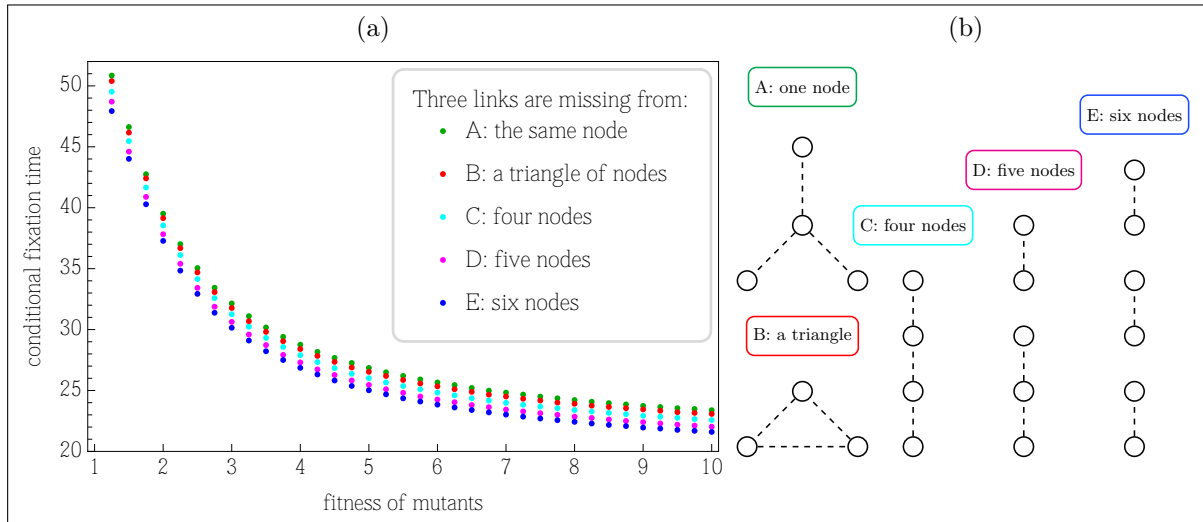


Figure 4.3: (a) Three links are missing from the complete graph of size eight. On all those five possible structures with 25 links, fixation time is plotted against the fitness of mutants. (b) The different possibilities to drop three links in a graph of size eight. For visualization, only the nodes with missing links are drawn. The dashed lines represent links that were omitted. Note that in these five structures, all the other 25 links are present.

Comparing only those structures, the variance in node degree seems to determine fixation time. Figure 4.3a indicates, that the more isolated some nodes are, the longer the process takes until absorption into the all-mutant state.

## 4.2 Influence of the "Five Links" on Fixation Time

In section 3.3.2, it was shown that the graph with four nodes and five links increases fixation time, compared to the ring. Now we analyze this structure, to find out whether the increase happens for slightly larger graphs as well. Figure 4.4 visualizes the average conditional fixation time on the ring of sizes four, six and eight in green. For the ring-structure with one link straight through, fixation time is plotted in purple.
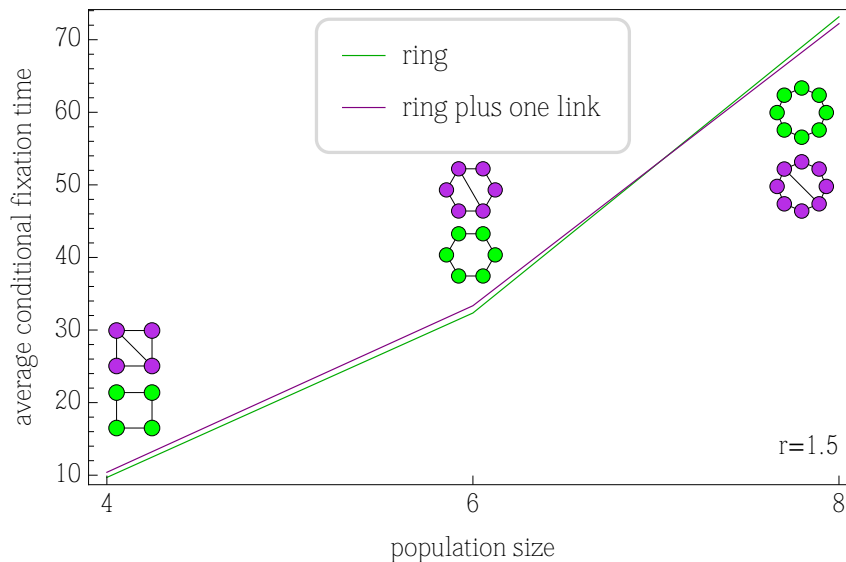


Figure 4.4: Simulated fixation time on the ring of sizes four, six and eight and the ring-like-structure with five, seven and nine links. A fitness $r = 1.5$ for mutants is used. Note that the lines are drawn solid only for a better visualization of the six simulated results and do not imply a continuous function here.

It can be seen in figure 4.4, that the increase compared to the ring is only present for sizes four and six. For size eight, the ring has a higher fixation time. Simulations were repeated for larger sizes 16 and 32. The larger rings showed a higher fixation time as well.
It seems that this effect is either an artifact of small graph size, or maybe, adding just one link to the ring is not the right way to compare them.

Therefore it would be interesting to analyze the structure with five links in other larger graphs. For example a well-mixed population with this structure attached to it, compared to a well-mixed population with a ring attached to it. Or a large graph consisting of repetitions of this structure, compared to a large lattice of the same size.

48

# 5 Discussion

This chapter summarizes the results and draws conclusions from our findings. At last, we will give an outlook to further research.

## 5.1 Summary and Conclusion

Recall that the aim of this thesis was answering the three questions phrased at the end of chapter 2. Question 1 asks whether every graph that differs from the complete graph, increases the fixation time of advantageous mutants. We were able to answer this analytically for graph size four. And so far, we did not find a counter-example by simulating the process on larger graphs. See the discussion on the next page for reasons that complicate analytical approaches.

Question 2 reads: given any graph structure, does the removal of one link lead to a higher fixation time? Figure 3.14 showed that there is a structure (the complete graph), for which the removal of a link leads to an increase in fixation time and there is another graph (the structure with four nodes and five links), for which removing a link leads to a decrease in fixation time. This is counter-intuitive and negates question 2, since the removal of a link apparently does not always increase fixation time.

Question 3 aims at accessing the relationship between fixation probability and fixation time. Given any graph, does a fixation probability that was increased by removing or adding links, necessarily lead to an increased fixation time? We can answer question 3 for population size four. Increasing the fixation probability in a given graph of size four, by removing or adding links, leads to an increase in fixation time. Given the ring for example, fixation probability increases by adding a link to receive the structure with five links. At the same time, fixation time is increased as well.

Figure 3.16 showed, why fixation takes longer on the ring than in the well-mixed population. Sojourn times in the states with one and three mutants are the same as on the complete graph. But the process on the ring stays in the two-mutant state for a longer time than the process in the well-mixed population. This is due to the fact that the probability to stay in state II is $T_{II,II} = \frac{1}{2}$ on the ring and only $T_{II,II} = \frac{1}{3}$ in the well-mixed population (see the transition matrices in equations (3.1) and (3.4)). Remarkably, those two transition probabilities do not depend on the fitness of the mutants.

In section 3.5, we analyzed the effective rate of evolution, which has been proposed by *Frean et al.* [2013], on the six graphs of size four. We saw in figure 3.21 that for intermediate mutation rates, evolution proceeds slowest on the star, compared to the other five structures of size four. This underlines the importance of fixation time, since by only looking at the former rate of evolution, one would conclude that evolution proceeds fastest on the star.

**Why have we not been able to show that the removal of one link from the well-mixed population always increases fixation time?**

For isothermal graphs, the fixation probability and the conditional fixation time both depend on the transition probabilities $t_i^{\pm}$. But their relationship is not trivial, because the fixation probability enters the conditional fixation time, see equation (2.5). And what further complicates the matter, is that for graphs that are not isothermal, conditional fixation time is not given by equation (2.5), as argued next.

The transition matrix of a non-isothermal graph generally does not have a tridiagonal shape, because the process can not be mapped to a simple birth-death process. Instead, several different states exist for each number of mutants. Therefore, the matrix has more than the $N + 1$ rows and columns that the transition matrix of an isothermal graph has. For example, the graph with four nodes and five links has 9 different states (see figure 3.8). The approach which we used for calculating the fixation time on the structure with five links yields a rational function in $r^{15}$ with coefficients that consist of up to 13 digits. Recall that this is only for a population size $N = 4$. This makes it impossible to compare the functions analytically, and it gets even worse for larger graph sizes.

Since this approach performs matrix multiplications and inversions, large transition matrices increase the computational effort to conduct these calculations. We therefore conclude that this analytical approach is not feasible for large graphs.

The general question 1, whether any graph that is different from the complete graph increases fixation time, remains to be proven or negated.

**Influence of the Variance of Node Degree**

By comparing the five structures with 8 nodes and 25 links in figure 4.3, one might speculate that the variance of the node degree distribution determines the mean conditional fixation time on a graph. However, the following table for graphs of size four disproves this speculation:

Table 5.1: Node degrees and variance of node degree for the six different graphs of size $N = 4$.

| Graph | Node degrees | Variance |
|---|---|---|
| Star | $\{3, 1, 1, 1\}$ | 1 |
| Line | $\{2, 2, 1, 1\}$ | 1/3 |
| Shovel | $\{3, 2, 2, 1\}$ | 2/3 |
| Five links | $\{3, 3, 2, 2\}$ | 1/3 |
| Ring | $\{2, 2, 2, 2\}$ | 0 |
| Complete graph | $\{3, 3, 3, 3\}$ | 0 |

Since the graphs in table 5.1 are ordered according to decreasing mean conditional fixation time, we see that the variance does not increase monotonicly with the fixation time. Instead, the line has a node degree variance of $\frac{1}{3}$, which is less than the $\frac{2}{3}$ of the shovel.

**Biological Application**

The Moran process with spatial population structure has many biological applications, since the habitats of populations are almost never well-mixed.

In experimental evolution, it is possible to control the environmental factors that affect a population. This is of biotechnological interest when a certain mutation needs to be fixed in a population to create or improve a pharmaceutical [*Moore and Arnold*, 1996; *Turner*, 2009]. By improvement, we mean inducing a resistance against a certain chemical or increasing the gene expression level for example. By placing the individuals (in that case, bacteria) as nodes of an amplifying graph, one increases the probability of fixation of a newly introduced mutant.

However, fixation time is increased as well. For intermediate mutation rates, evolution proceeds slower on those graphs, see *Frean et al.* [2013] and chapter 3.5.

Thus, a trade-off between probability and time needs to be taken into account, which can be accomplished by looking at the effective rate of evolution.

As a nice feature of the process on a graph, the optimal starting node for shortest average fixation time of a mutant can be found via simulations.

The invasion process may also correspond to the spreading of ideas in a social network. For example the star represents one influential person with many friends. The "fitness" could measure how persuasive an individual is. The resident population is more likely to become influenced by an idea, the more persuasive the invaders are.

As we have seen, the probability for a new idea to become fixed in a star network, is very high. But it takes a long time, because all information is flowing via the individual at the center which changes its opinion a lot.

It has been shown by *Barabási et al.* [2002] that scientific collaboration networks are scale-free. A scale-free graph is characterized by a few "hub nodes" that have many links and many nodes that have just a few links. A logarithmic plot of the node degree distribution looks like a straight line. The evolution of the network, that is the positioning of links onto the graph, follows a pattern that is called preferential attachment. Preferential attachment can be simulated with the Barabási-Albert model, where a graph is constructed by adding a new node at every step [*Albert and Barabási*, 2002]. Links from the new node to the existing nodes are set with probability proportional to the node degree of the respective existing node. Therefore, nodes with many neighbors are more likely to get a new neighbor. This concept is also called "the rich get richer".

For the scientific network, this means that researchers with a lot of collaborators are more likely to be introduced to a new collaborator.

Also, many biological networks like metabolic and protein networks are scale-free [*Albert and Barabási*, 2002], which is useful because scale-free networks are more robust against random mutations or external influences than random graphs [see *Callaway et al.*, 2000]. Note however, that they are susceptible to attacks against their hub nodes.

*Lieberman et al.* [2005] have shown that scale-free networks are amplifiers of selection. Therefore, the probability for a novel idea or concept to take over the whole network is very high. But it may take a long time.

## 5.2   Outlook

Throughout this thesis, we used the mean conditional fixation time for comparing the time until absorption in different graph structures. But the mean is only an appropriate representative of the distribution, if the distribution is symmetric. Therefore, as a prospect to further studies, let us have a look at the simulated distributions.

In figure 5.1, the distribution of the conditional fixation time is plotted for the six graphs of size four. Recall that on all these graphs, the mean fixation time is higher for neutral evolution than for strong selection.
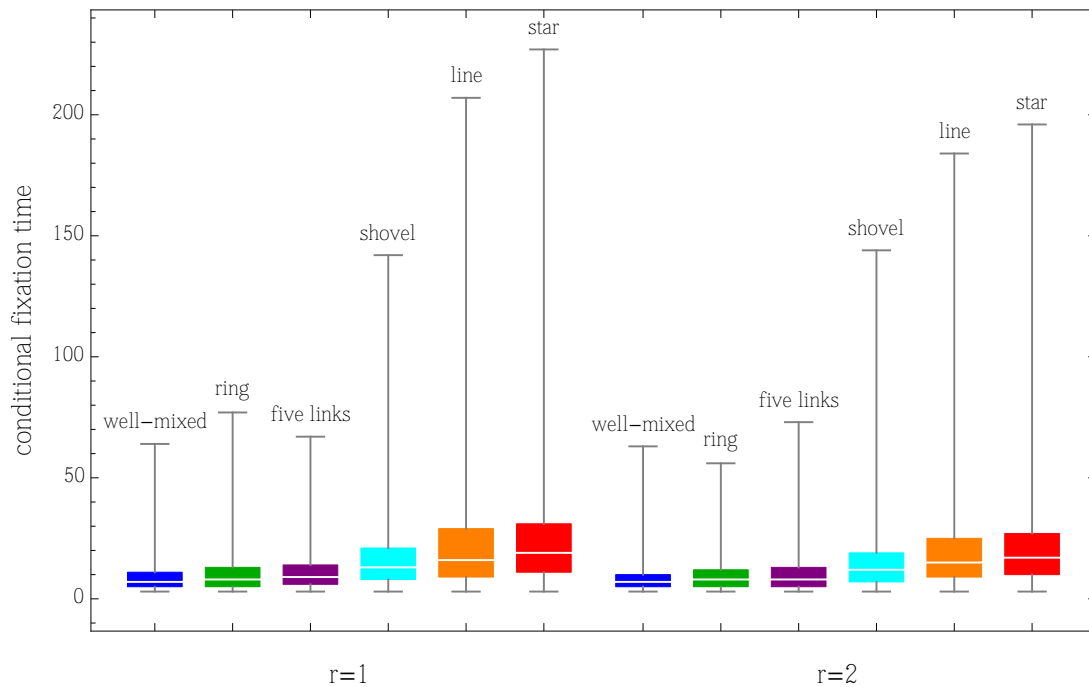


Figure 5.1: Box-Whisker-Chart of the distributions of the conditional fixation on the six graphs of size $N = 4$. In the left part, neutral evolution is modeled by a fitness value $r = 1$, whereas in the right part, selection is present with $r = 2$. We conducted $10^5$ independent realizations for every graph.

It can be seen in figure 5.1 that the distributions are right-skewed. That is, there are many small values close to the mean and just a few very high values. This is true for $r = 1$, $r = 2$ and for even stronger selection as well, which is not included in this figure.

We conclude that the median would be the more appropriate measure for future comparison of fixation times, due to the skewness of the distributions. But this is only feasible computationally, since the median is calculated from data.

One possible next step is to further analyze the distributions. Especially the higher moments like the variance and the skewness will be of interest to provide information about the distributions.

Another intention is accessing the effect of the "five links" on fixation time in larger populations by conducting simulations. One way to do that, is by comparing a large two-dimensional lattice (which can be seen as many rings side by side) to a lattice of the same size, where the rings have one additional link straight through. The latter structure therefore looks like many "five link-structures" glued together.
Additionally, one could create a large well-mixed population with a ring attached to it in one case, and a structure with five links attached to it in the second case. This could be useful in finding out, whether this is a network motif that has an important influence on fixation time.

We have seen that the effects of local graph structure on the mean fixation time can be surprising and sometimes even counter-intuitive. A lot of open questions remain. Therefore, the need for simplifying approaches that make analytical calculations of fixation time on networks more feasible is ever so obvious.

# References

Abramson, G. and Kuperman, M.: *Social games in a social network.* Physical Review E, 63:page 030901 [2001].

Albert, R. and Barabási, A.-L.: *Statistical mechanics of complex networks.* Review of Modern Physics, 74:pages 47–97 [2002].

Allen, L.J.S.: *An Introduction to Stochastic Processes with Applications to Biology.* Pearson Education, New Jersey [2003].

Altrock, P. M.; Traulsen, A. and Galla, T.: *The mechanics of stochastic slowdown in evolutionary games.* Journal of Theoretical Biology, 311:pages 94–106 [2012].

Barabási, A.L.; Jeong, H.; Néda, Z.; Ravasz, E.; Schubert, A. and Vicsek, T.: *Evolution of the social network of scientific collaborations.* Physica A, 311:pages 590–614 [2002].

Broom, M. and Rychtář, J.: *An analysis of the fixation probability of a mutant on special classes of non-directed graphs.* Proceedings of the Royal Society A, 464:pages 2609–2627 [2008].

Callaway, D. S.; Newman, M. E. J.; Strogatz, S. H. and Watts, D. J.: *Network robustness and fragility: percolation on random graphs.* Physical Review Letters, 85:pages 5468–5471 [2000].

Ewens, W. J.: *Mathematical Population Genetics. I. Theoretical Introduction.* Springer, New York [2004].

Frean, M.; Rainey, P. and Traulsen, A.: *The effect of population structure on the rate of evolution.* Proceedings of the Royal Society B, 280(1762):page 20130211 [2013].

Grinstead, C. M. and Snell, J. L.: *Introduction to Probability.* American Mathematical Society [1997].

Karlin, S. and Taylor, H. M. A.: *A First Course in Stochastic Processes.* Academic, London, 2nd edition edition [1975].

Lieberman, E.; Hauert, C. and Nowak, M. A.: *Evolutionary dynamics on graphs.* Nature, 433:pages 312–316 [2005].

Moore, J C and Arnold, F H: *Directed evolution of a para-nitrobenzyl esterase for aqueous-organic solvents.* Nature Biotechnology, 14:pages 458–467 [1996].

Nowak, M. A.: *Evolutionary Dynamics.* Harvard University Press, Cambridge MA [2006].

Nowak, M. A. and May, R. M.: *Evolutionary games and spatial chaos.* Nature, 359:pages 826–829 [1992].

Nowak, M. A.; Tarnita, C. E. and Antal, T.: *Evolutionary dynamics in structured populations.* Philosophical Transactions of the Royal Society B, 365:pages 19–30 [2010].

Ohtsuki, H.; Hauert, C.; Lieberman, E. and Nowak, M. A.: *A simple rule for the evolution of cooperation on graphs.* Nature, 441:pages 502–505 [2006].

Santos, F. C. and Pacheco, J. M.: *Scale-free networks provide a unifying framework for the emergence of cooperation.* Physical Review Letters, 95:page 098104 [2005].

Traulsen, A. and Hauert, C.: *Stochastic evolutionary game dynamics.* Heinz Georg Schuster, editor, *Reviews of Nonlinear Dynamics and Complexity*, volume II, pages 25–61. Wiley-VCH, Weinheim [2009].

Traulsen, A.; Sengupta, A. M. and Nowak, M. A.: *Stochastic evolutionary dynamics on two levels.* Journal of Theoretical Biology, 235:pages 393–401 [2005].

Turner, N.J.: *Directed evolution drives the next generation of biocatalysts.* Nature Chemical Biology, 5:pages 567–573 [2009].

# Acknowledgements